

An overview of the influence of hydrodynamics on the spatial and temporal patterns of calanoid copepod communities around Taiwan

GAEL DUR^{1,2}, JIANG-SHIU HWANG^{1*}, SAMI SOUSSI², LI-CHUN TSENG¹, CHENG-HAN WU¹, SHIH-HUI HSIAO¹ AND QING-CHAO CHEN³

¹INSTITUTE OF MARINE BIOLOGY, NATIONAL TAIWAN OCEAN UNIVERSITY, 2 PEI-NING ROAD, KEELUNG, TAIWAN 20224 ROC, ²ECOSYSTEM COMPLEXITY RESEARCH GROUP, STATION MARINE DE WIMEREUX, UNIVERSITÉ DES SCIENCES ET TECHNOLOGIES DE LILLE, CNRS-FRE 2816 ELICO, 28 AV. FOCH, 62930 WIMEREUX, FRANCE AND ³SOUTH CHINA SEA INSTITUTE OF OCEANOLOGY, CHINESE ACADEMY OF SCIENCE, 164 WEST XINGANG ROAD, GUANGZHOU 510275, CHINA

*CORRESPONDING AUTHOR: jshwang@mail.ntou.edu.tw

Received May 15, 2006; accepted in principle August 4, 2006; accepted for publication October 27, 2006; published online December 6, 2006

Communicating editor: K.J. Flynn

*Taiwan waters are oceanographically complex, being characterized by different water masses in the East China Sea, the South China Sea, the Pacific Ocean and the Taiwan Strait, which form contiguous but distinct ecosystems. These ecosystems interact one with another through complex and strong water circulations. The present work investigates the relatively few studied interactions between the local copepod communities and the heterogeneous hydrodynamical regimes. Gathering data from 53 cruises carried out since June 1998 to October 2004 all around Taiwan, this study leads to the mapping of eleven local calanoid assemblages taking into account the physical properties of the environment in which they appeared and the characteristics of their indicator species. Three of these identified assemblages were located in the tropical waters, southwest of Taiwan. First, the assemblage of the 2001 South China Sea sampling cruises revealed a tropical community dominated by *Acrocalanus gracilis* and *Undinula vulgaris*. In the other cluster, tropical calanoid species such as *Labidocera detrunccata*, *Centropages calaninus* and *A. monachus* were found. The eight other assemblages were associated with the seasonal dynamics of the water masses north of Taiwan. Although the seasonal characteristics in the north can be subtle, the demarcation between these assemblages was clear. The early spring community is dominated by *Calanus sinicus* and followed by *Temora turbinata* since the beginning of summer. September marks a transition period to a new community characterized by the indicator species *A. gibber*. When the north-easterly monsoon prevails in winter, it is the turn of the community of northern common species such as *Paracalanus parvus* and *Euchaeta concinna* to prevail. In the mean time, *C. sinicus* starts its intrusion from the Yellow Sea and the East China Sea towards the northwest of Taiwan. Thus, according to our results, identified assemblages appear to be good indicators of different, distinctive, water masses.*

INTRODUCTION

Marine ecosystem functioning is strongly dependent on zooplankton community structure and succession. For more than two decades, the intimate relationship between the structuring of zooplankton communities

and large-scale physical processes such as the transport of water masses, by currents has been revealed in various ecosystems (Gowen *et al.*, 1998; Lopez *et al.*, 1999; Gomez *et al.*, 2000; Hwang *et al.*, 2004b, 2006; Berasategui *et al.*, 2006; Sanders, 1987; Turner, 2004). Hence, the interpretation of the macro-scale distribution

patterns of zooplankton populations related to their water mass properties and their trends of transport is fundamental to the understanding of pelagic ecosystem dynamics (Boucher *et al.*, 1987; Kouwenberg, 1994; Beaugrand, 2005; Hwang and Wong, 2005).

Studies on the general characteristics of copepods associated with the hydrodynamics and the hydrological features in the vicinity of Taiwan revealed that this oceanic region is filled with complex dynamic processes (Hwang *et al.*, 2004a, b, 2006; Hwang and Wong, 2005). First of all, the island of Taiwan is surrounded by different water masses (East China Sea, Pacific Ocean, Taiwan Strait and South China Sea) which constitute continuous but distinct ecosystems: tropical in the south, subtropical in the north and oceanic in the east. Moreover, the interaction between those ecosystems is furthered by strong hydrodynamic activity. The water circulation is influenced among other factors, by a semi-diurnal tide regime, the presence of strong currents (Kuroshio current and Chinese coast current) and its interaction with other factors including monsoon winds (two dominant monsoon regimes, northeast during winter and southwest during summer). The water circulation presents seasonal variation and has been the subject of numerous hydrological studies (Jan *et al.*, 1995, 2002; Lee and Chao, 2003; Tseng and Chen, 2003). These physical characteristics make Taiwan an ideal location for studies of the biodiversity of planktonic copepods (Hwang *et al.*, 2000b, 2004a).

The eastern Taiwan oceanic waters are influenced by the Kuroshio Current whose path parallels the shoreline, showing no obvious seasonal variation. As soon as the Kuroshio Current reaches the northern part of the island, seasonal patterns can be observed. During the southwesterly monsoon (June–September), the Kuroshio main stream is redirected towards the east. This branch forms a counter clockwise circulation which disappears during the northeasterly monsoon, from October to April (Liang *et al.*, 2003). The Kuroshio on-shelf intrusion in winter is joined by the Taiwan Strait outflow and they primarily flow northward (Liang *et al.*, 2003; Tseng and Shen, 2003). In the northern part of this Strait (northwest of Taiwan) and the southern edge of the East China Sea, water circulation is strongly influenced by monsoon winds. During the north-east monsoon period, the temperate and nutrient rich China Coastal Current flows southward through the western part of the Taiwan Strait, but in the eastern part of the strait, a warm and salty branch of the Kuroshio flows northward (Liang *et al.*, 2003). During the rest of the year, particularly in summer when the strength of the southwesterly monsoon increases, the current flows primarily northeastwards. The current maintains this direction in the southern part

of the Taiwan Strait regardless of the seasons (Jan and Chao, 2002). On the southern coasts, the Kuroshio penetrates into the South China Sea in the Luzon Strait regardless of the season. It interacts with the South China Sea current and forms a clockwise flow. Most of the water in this clockwise current returns to the Kuroshio at the tip of southern Taiwan in summer (Liang *et al.*, 2003).

The hydrodynamic regime generates heterogeneity in water masses, as well as strong seasonal variation. For example, the temperature at 5-m depth varies between 10.6°C and 31.3°C (Lee *et al.*, 2005). This variability leads to a rich planktonic copepod fauna in the coastal and offshore waters of Taiwan which is constantly reorganized throughout the year.

Among zooplankton groups, copepods dominate the mesozooplankton in Taiwan waters, both in terms of species diversity and numerical abundance (Hwang *et al.*, 2000b, 2004a, 2006; Lo *et al.*, 2004b; Shih and Young, 1995). Indeed, with the richness of their species (208 species according to Shih *et al.* (Shih *et al.*, 2000) and Lo *et al.* (Lo *et al.*, 2004c) with many more species again in a recent review (C.T. Shih, National Taiwan Ocean University, unpublished data)), they are undoubtedly the largest and most diverse group (Hwang *et al.*, 2003). As their abundance and distribution are known to be influenced by hydrographic conditions (Boucher, 1984; Shih and Chiu, 1998; Hwang *et al.*, 2000b, 2004a, 2006), it has been suggested that they might be good biological indicators for water masses (Zheng *et al.*, 1992; Beaugrand *et al.*, 2002; Hwang and Wong, 2005; Hwang *et al.*, 2006). Forecasting changes in copepod fauna with a direct mechanistic understanding of the processes that contribute to these changes is, therefore, important in confirming the idea that copepod species composition, assemblages or associations should be predictable and useful in detecting patterns of water mass flow (Boucher *et al.*, 1987; Zheng *et al.*, 1992; Hsieh *et al.*, 2004; Lan *et al.*, 2004; Hwang and Wong, 2005; Hwang *et al.*, 2006). Furthermore, the high diversity of water masses surrounding Taiwan provides a good testbed for concepts involving the linking of copepod assemblages to physical oceanography.

During the last decade, studies on copepods in the vicinity of Taiwan have become more frequent. However, they are all local studies with emphasis on species composition (Hsieh and Chiu, 1998; Shih and Chiu, 1998; Lo *et al.*, 2001; Chang and Fang, 2004; Lan *et al.*, 2004; Lo *et al.*, 2004a), taxonomy and distribution of new species (Lin and Ho, 1998; Chen and Hwang, 1999; Chen *et al.*, 2004; Hsiao *et al.*, 2004), behaviour at small scale (Hwang and Turner, 1995; Strickler and Hwang, 1999) and on feeding ecology (Hwang *et al.*,

1998; Wong *et al.*, 1998; Wu *et al.*, 2004; Lo *et al.*, 2004c). Only a few studies focused on the relationship between species patterns and characteristics of water masses (Shih and Chiu, 1998; Hwang *et al.*, 2004b, 2006; Liu *et al.*, 1992; Lo *et al.*, 2004b; Hsieh *et al.*, 2005; Hwang and Wong, 2005). However, these too were short-term studies [except for Hwang *et al.* (2004b) with a 3-year study and Hwang *et al.* (2006) with a 5-year study] conducted in restricted areas off Taiwan and none of them integrated data from different ecosystems surrounding the island.

From a general point of view, this current study investigates the potential for using copepods as indicators of water masses, specifically taking the Calanoida as an example. Precisely, the goal of our study is to assess the influences of hydrological conditions on calanoid copepod assemblages in Taiwan waters. In order to reach this goal, a database was used from entire sets of copepod samples collected and analysed from tropical and subtropical Taiwan waters during the last decade. The study of large-scale plankton assemblage dynamics requires appropriate statistical approaches (Souissi *et al.*, 2001; Anneville *et al.*, 2002). In the present study, calanoid assemblages with their respective key species were identified by the adaptation of a multivariate analysis as developed similarly by Souissi *et al.* (Souissi *et al.*, 2001). This method involved hierarchical clustering, determination of species associations and an analysis of their pattern of occurrence related to the hydrodynamics of the area studied. It thus brought sufficient information to answer the following questions: (i) Which calanoid species assemblages and indicator species have occurred in tropical and subtropical Taiwan waters since 1998? and (ii) Which were the environmental conditions that characterized each of them?

METHOD

Data origin

Copepod Database

Study area and sampling method. Biological data used in this study have been compiled from the results of several years of investigations carried out at four sampling sites around Taiwan: (i) North of Taiwan off Danshuei estuary coastal waters (hereafter referred to as Pa-Li), (ii) North of Nuclear Power Plant waters (hereafter referred to as NPP), (iii) South China Sea (hereafter referred to as SCS) and (iv) in the vicinity of Peng-Hu (Fig. 1). These areas represented the most dynamic water masses which surround the island.

The two northern sites constituted the location of intensive sampling efforts in the northern sub-tropical waters of Taiwan. The South China Sea and Peng-Hu data stemmed from punctual investigations carried out in southwestern tropical waters.

The site of Pa-Li covered the plume and adjacent waters of the largest river of northern Taiwan: the Danshuei River. Moreover, this area is the meeting point of the East China Sea and the Taiwan Strait (Fig. 1A). The 19-station monitoring program was spread over a period of ~6 years from October 1998 to July 2004, with 26 sampling cruises (Table I).

The Nuclear Power Plant monitoring program lasted from November 2000 to October 2004 and included a total of 17 sampling cruises (Table I). Copepods were sampled at 28 stations which define transects from inlet and outlet waters around the two nuclear power plants and the Hwang River (Fig. 1B).

The third site in the South China Sea covered a large oceanic site with 56 stations (15°–25°N, 113°–121°E) mainly surrounded by waters of Taiwan, Philippines, Hong Kong and China in the South China Sea (Fig. 1). Within this area, fifteen cruises were carried out from October 1998 to October 2002, but the sampled stations were different for each sampling cruise (Table I).

With its 34 stations, the last sampling site of interest (Peng-Hu) covered an area between the Taiwan Bank and the Yunchan rise, including the Peng-Hu channel (Fig. 1D). The data from this area came from only one cruise carried out in June 1998 (Table I).

The treatment of samples from arrival on board to the final database was the same for all areas studied. All planktonic copepod specimens obtained from each haul were preserved in 5% buffered formalin solution immediately after collection. The procedure of subsampling, species identification and counting are similar to each other and to those described in (Hwang *et al.*, 1998, 2006; Wong *et al.*, 1998; Hsiao *et al.*, 2004; Lo *et al.*, 2004b; Wu *et al.*, 2004; Hwang and Wong, 2005).

Selection of a sub-set of data

To create a homogeneous and coherent data base, as far as possible avoiding any possible limitation of further analysis, data from similar sampling methods were used in this study. For each site, we retained the data obtained for the upper layer (0–5 m), sampled by oblique tows of a NORPAC zooplankton net (333- μ m mesh size, 0.45-m diameter and 180 cm in length) at a speed of 2 knots for 10 min. Table I presents the characteristics of the final set of cruises selected for further analysis. A focus on the upper layer was also chosen due to the physical importance of this zone, as it

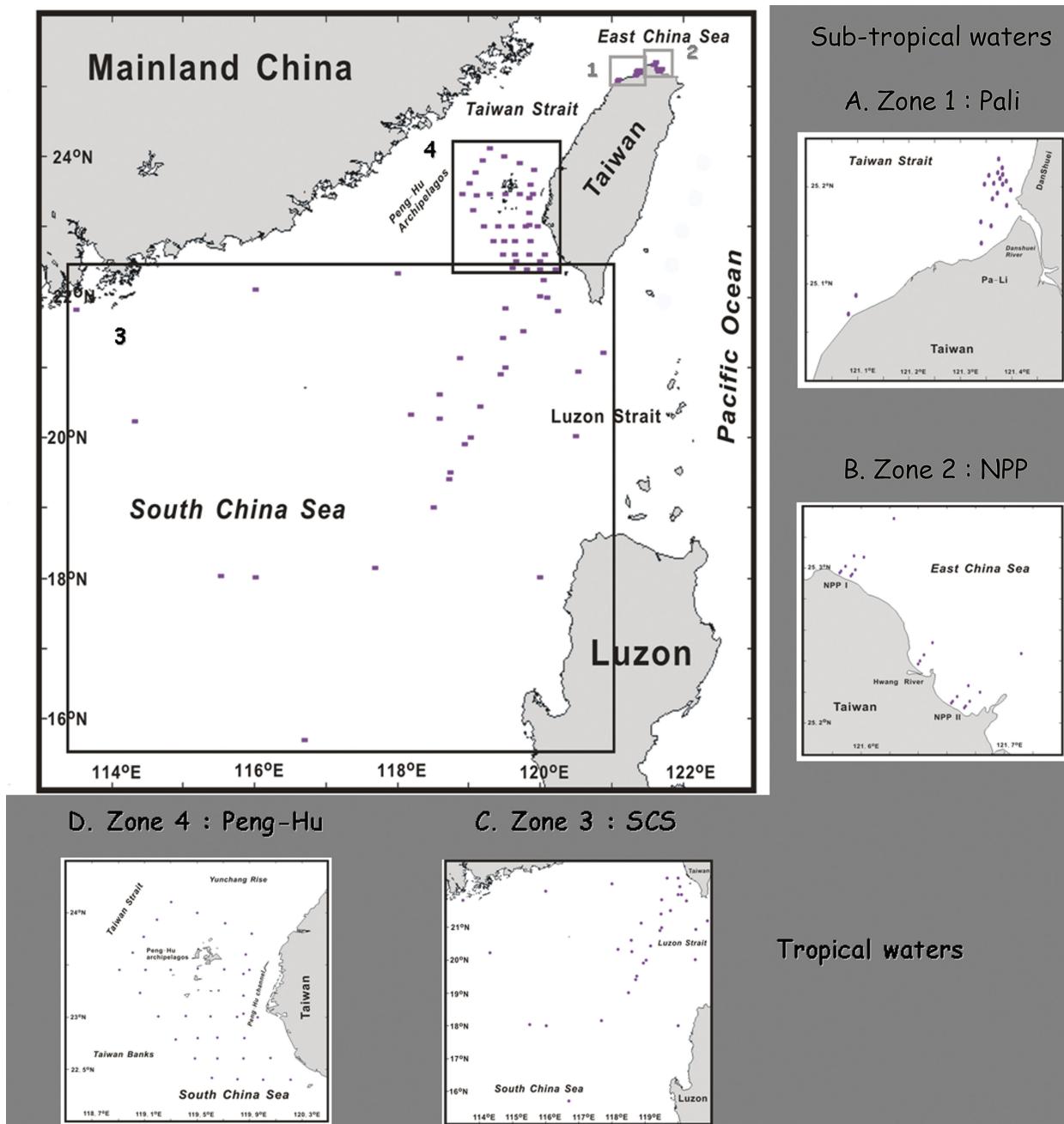


Fig. 1. Chart showing waters surrounding Taiwan and the sampling zones chosen for the analysis. The sampling sites in sub-tropical waters (northern coast of Taiwan, in grey) correspond to long-term monitoring programs off the Danshuei Estuary and the coastal waters near the Northern Taiwan Nuclear Power Plants (sampling stations are transects from inlet to outlet waters). Additional samplings in the Taiwan Strait (southern part) and South China Sea were considered as a reference to tropical waters.

is mostly influenced by water movements at the surface (0–10-m depth).

The Calanoida were chosen considering the fact that (i) calanoid copepods are relatively easier to identify than other orders, and therefore they have been identified at species level in the different samples and

(ii) calanoids are commonly the most abundant group of copepods. Mauchline (Mauchline, 1998) gave a general approximate range of 30–60 ind. m⁻³ for the 0–100-m depth layer in oceanic waters. This is similar to our data; the calanoid species represented more than 80% of the identified species in a raw dataset.

Table I: General characteristics of the four sampling areas

Area studied	Number of stations	Number of cruises	Period covered	Season sampled	Calanoid species
Pa-Li	19	25	October 1998–July 2004	All	79
Taiwan Nucler Power Plant (NPP)	28	17	November 2000–October 2004	All	84
South China Sea (SCS)	34	10	October 1998–October 2002	All	67
Peng-Hu Archipelagos	35	1	June 98	Spring	51

The number of calanoid species is based on the analysis of surface sampling (0–5 m) using a 333- μ m mesh net.

Moreover, the voluntary delimitation of data derived from a standard NORPAC zooplankton net of 333 μ m, could have provided biased data concerning the size range. Smaller calanoid copepods, and representatives of entire orders, such as the Poecilostomoida and the Cyclopoida, the second and third most important copepod orders observed in the entire dataset, might have been underrepresented here.

Even after such sub-selection, the calanoid species matrix was quite large, merging the 1029 records (number of individual samples) of the 192 identified calanoid species' abundance from the four studied areas.

Data analysis

Cluster analysis and characterization of indicator species

To simplify the data analysis, the calanoid copepod abundances were averaged for each sampling cruise. Therefore, the cluster analysis was applied to the resulting matrix composed of mean abundances of all calanoid species ($n = 192$) as variables and 53 sampling cruises in the different areas as observations.

The matrix was first log-transformed [$\log(x + 1)$] in order to decrease the weight of high-abundance figures in some species, then a hierarchical classification of the samples was applied to the new matrix, using the Bray–Curtis similarity coefficient and clustering strategy of flexible links as developed by Souissi *et al.* (Souissi *et al.*, 2001). Further mathematical details of the technique and subsequent treatments are given in Souissi *et al.* (Souissi *et al.*, 2001).

Descriptions of the different clusters that emerged among the eleven first hierarchical levels were selected. This was thought to be appropriate to answer our objective to link the copepod assemblage to hydrodynamics, providing optimal mapping for the ecological characteristics of the clusters.

After mapping the sample groups, indicator species for each cluster were further identified using the indicator value index (hereafter referred to as IndVal) as proposed by Dufrene and Legendre (Dufrene and Legendre, 1997). The choice of this index was directed by its

proven effectiveness (Souissi *et al.*, 2001; Anneville *et al.*, 2002, 2004). As in Dufrene and Legendre (Dufrene and Legendre, 1997) and Souissi *et al.* (Souissi *et al.*, 2001), the arbitrary threshold IndVal value of 25% was retained for characterizing indicator species of the calanoid copepod assemblages. All steps of this method were computed using Matlab V6.1 software (Mathworks Inc.).

Characterization of environmental conditions

First, we identify the spatial and temporal characteristics of each cluster of samples obtained by the previous method so as to, when possible, link the assemblages with water mass dynamics considering surface current speeds and sea surface temperature data. Current data came from the major oceanographic data base in Taiwan: Ocean Data Bank (ODB). ODB is provided by the National Center for Ocean research of Taiwan (www.ncor.ntu.edu.tw). The current data we have at our disposal covered a period from January 1985 to December 2003 and were supplemented by satellite images of sea-surface temperatures (SSTs) at the time of the cruises. These temperature data providing large scale patterns of the marine environment came from the primary sensor carried onboard the National Oceanic and Atmospheric Administration (NOAA) polar orbiting satellite, employing an advanced very-high-resolution radiometer (AVHRR). All available images corresponding to the chosen assemblages were used and compared to CTD data recordings during the samplings. Those were compared with the results of the cluster analysis of taxa.

Characteristic seasonal distribution of key species in the north of Taiwan

For this analysis, patterns in seasonal distribution and abundance of four characteristic species, one per season, were visualized by contours of abundance. The Surfer V6 software (Goldensoftware Inc.) was used to generate inverse distance to power grids and map the seasonal density and distribution of the four seasonal typical species. As only Pa-Li and NPP sampling areas exhibited a sufficiently detailed data set to realize this work, we exclusively focused on the seasonal variation along the northern Taiwan coast. The sampling during

2002 was complete; consequently this year was used to illustrate seasonal patterns of the key species.

RESULTS

Cluster analysis

The organization of sampling cruises within clusters was analysed following the different hierarchical levels until the twelfth. Eleven coherent groups revealed were chosen for their identification and ecological interpretation. The description of each cluster, with its spatio-temporal patterns and its associated water masses, was first investigated. Secondly, we made the link between the feature of the indicator species revealed for each cluster and the hydrographical conditions.

Seasonal, interannual and site origin of the cluster

Table II provides information about the spatial and temporal (seasonal and inter-annual) pattern of the different groups. As each cluster of samples was associated with a calanoid assemblage, these spatio-temporal indications (i.e. sampling site, month and year) give indications for the description of the water mass from which the calanoid copepod assemblage was collected.

From the first cut-off level obtained at 140% of dissimilarity (Fig. 2), the periods at colder regimes (mean $T = 19.2^{\circ}\text{C} \pm 3^{\circ}\text{C}$) were separated from the other samplings (mean $T = 25.2^{\circ}\text{C} \pm 3^{\circ}\text{C}$). These 'cold' period assemblages merged only with samplings at northern Taiwan sites (assemblages 1 and 2, Table II). Among the six sampling cruises gathered in assemblage 1 (A4_1), only one was from NPP; the five others were from Pa-Li (Table II). A higher proportion of samplings were restricted to the winter months (Dec–Feb) to which autumnal (November) samplings from Pa-Li were added. The sampling years corresponding to this assemblage were spread from 1998 to 2004. This cluster thus appeared as the early northeasterly monsoon community in the Northern Coastal Waters of Taiwan. The second cluster obtained at the same hierarchical level (A4_2) distinguished the sampling campaign achieved in the Pa-Li area during 2000 (Table II, Fig. 2). The extraction of only one sampling cruise presumed the presence of a particular calanoid community linked to a specific hydrographical condition in this region during this period.

At the second cut-off (125% of dissimilarity) emerged a large cluster Ib which gathered subclusters 3, 4, 5 and 6 (Fig. 2). Except for cluster 5, IIa regrouped the data from tropical water samplings (Table II). The third assemblage (A5_2) revealed dissimilarity at ~85%

(Fig. 2) and included the samplings carried out around the Peng-Hu archipelagos in June 1998 and principally Autumn (Sep–Nov) South China Sea's sampling. Moreover, these sampling cruises, A5_2 aggregated also two other samplings from the South China Sea: one in March 1999 and one in December 1998 (Table II). The three following clusters (4, 5 and 6) are separated respectively at the sixth and seventh hierarchical levels (~75%). Cluster 4 gathered together all samplings carried out in the SCS during 2001, whereas both clusters 5 and 6 are representative of single sampling cruises. The samplings were carried out in NPP during May 2002 for cluster 5 and in SCS during July 1999 for cluster 6. As for the second group (A4_2), these assemblages suggest the presence of a particular calanoid community during these sampling periods.

Cluster 7 that appeared after the third cut-off, contained three recent samplings (2001–2003–2004) exclusively from Pa-Li. These sampling cruises remained grouped until the 24th level where the one from September 2003 is separated from the two summer sampling cruises. This cluster has been kept as it was revealed at the third level and associated with the south-westerly monsoon regime.

Northern autumnal and winter samplings from 2000 to 2004 were merged in cluster 8 (Table II), resulting in 70% dissimilarity (Fig. 2). Cruises from NPP represented a higher proportion in the cluster with six investigated months opposed to only two for Pa-Li. This period of the year corresponded to the ascending phase until the northeasterly monsoon prevailed.

On the following hierarchical level (No. 10, ~60% dissimilarity), cluster 9 was separated from the rest of the sampling cruises (Fig. 2). It comprised only the spring (Mar–May) investigations carried out at the northern sites from 2000 to 2004. The origins of the cruises were evenly shared between Pa-Li and NPP. Higher relative proportions were found for the cruises in Pa-Li in April (Table II). The period associated with this cluster corresponds to the transition between the two (NE and SW) monsoons. Therefore, the group was hereafter associated with such events and defined as the NE–SW monsoon transition community.

Cluster 10 was isolated by the cluster analysis at the 12th hierarchical level (~55%, Fig. 2). This one assembled five sampling cruises carried out in northern Taiwan coastal waters, three during 2002, one during June 2003 in Pa-Li and one during March 2002 in the waters off NPP. The spatial origin was primarily a north-western area (i.e. Pa-Li), representing 80% of the cruises (Table II). Spring 2002 was the principal season represented in this cluster (Table II).

Table II: Content description of the 11 assemblages obtained at various levels of resolution (from the 3rd to the 10th level)

Assemblage	Sampling area	Sampling month	Sampling year
No. 1 A4_1 (6)	Pali (83%)	February (17%)	1999 (17%)
		November (33%)	1999 (16.5%)–2001 (16.5%)
	NPP (17%)	December (33%)	1998 (16.5%)–2003 (16.5%)
		January (17%)	2004 (17%)
No. 2 A4_2 (1)	Pali (100%)	March (100%)	2000 (100%)
No. 3 A5_2 (7)	SCS (86%)	March (14%)	1999 (14%)
		September (14%)	2002 (14%)
		October (28%)	1998 (14%)–2002 (14%)
		November (14%)	1999 (14%)
		December (14%)	1998 (14%)
	P-H (14%)	June (14%)	1998 (14%)
No. 4 A6_2 (3)	SCS (100%)	March (33.3%)	2001 (33.3%)
		June (33.3%)	2001 (33.3%)
		October (33.3%)	2001 (33.3%)
No. 5 A7_2 (1)	NPP (100%)	May (100%)	2002 (100%)
No. 6 A7_2 (1)	SCS (100%)	July (100%)	1999 (100%)
No. 7 A3_2 (3)	Pali (100%)	June (33.3%)	2001 (33.3%)
		July (33.3%)	2004 (33.3%)
		September (33.3%)	2003 (33.3%)
No. 8 A8_2 (9)	Pali (33.3%)	September (11.1%)	2000 (11.1%)
		December (22.2%)	2000 (11.1%)–2002 (11.1%)
	NPP (66.7%)	January (11.1%)	2003 (11.1%)
		October (33.3%)	2001 (11.1%)–2002 (11.1%)–2004 (11.1%)
		November (11.1%)	2000 (11.1%)
		December (11.1%)	2003 (11.1%)
No. 9 A10_2 (7)	Pali (57%)	April (43%)	2001 (14.3%)–2003 (14.3%)–2004 (14.3%)
		May (14%)	2000 (14%)
	NPP (43%)	March (14.3%)	2001 (14.3%)
		April (14.3%)	2003 (14.3%)
		May (14.3%)	2001 (14.3%)
No. 10 A12_2 (5)	Pali (80%)	March (20%)	2002 (20%)
		April (20%)	2002 (20%)
		June (40%)	2002 (20%)–2003 (20%)
	NPP (20%)	March (20%)	2002 (20%)
No. 11 A12_1 (10)	Pali (50%)	May (10%)	2001 (10%)
		August (10%)	2001 (10%)
		September (10%)	2002 (10%)
		October (20%)	1998 (5%)–1999 (5%)
	NPP (50%)	May (30%)	2004 (10%)
		July (10%)	2002 (3.3%)–2003 (3.3%)–2004 (3.3%)
		August (10%)	2001 (10%)

The description includes the label of the assemblage and the number of the sampling cruise—each assemblage regroups in brackets (column 1), their spatial origin (column 2) and their sampling date (month, column 3; year, column 4). The relative proportions of the sampling in each assemblage are presented in parentheses (for example, the assemblage A4_1 provides 83% of the sampling realized in Pali, among which 17% were carried in February 1999, 16.5% in November 1998, 16.5% in November 2001, 16.5% in December 2008 and 27% in December 2003). The label of each assemblage $A_{i,j}$ represents the i th hierarchical level and the j th new cluster ($j = 1$ or 2).

Finally, cluster 11 that emerged also at the 12th hierarchical level, comprised 10 cruises between the two northern sites (Pa-Li and NPP). The sampling period encompassed by these regrouped investigations covered samplings from 1998 to 2004. The seasonal scale covering samplings of this cluster corresponded to the south-westerly monsoon (May–October). This assemblage was linked to this climatic event.

Classification and description of calanoid assemblages

Following the identification of their spatio-temporal distribution, we investigated the calanoid assemblage revealed at the successive hierarchical level, focusing on their identified indicator species as well as the mean value of temperature (Table III). Moreover, the hydrodynamic conditions associated with each assemblage, were taken into consideration, that is, sea surface

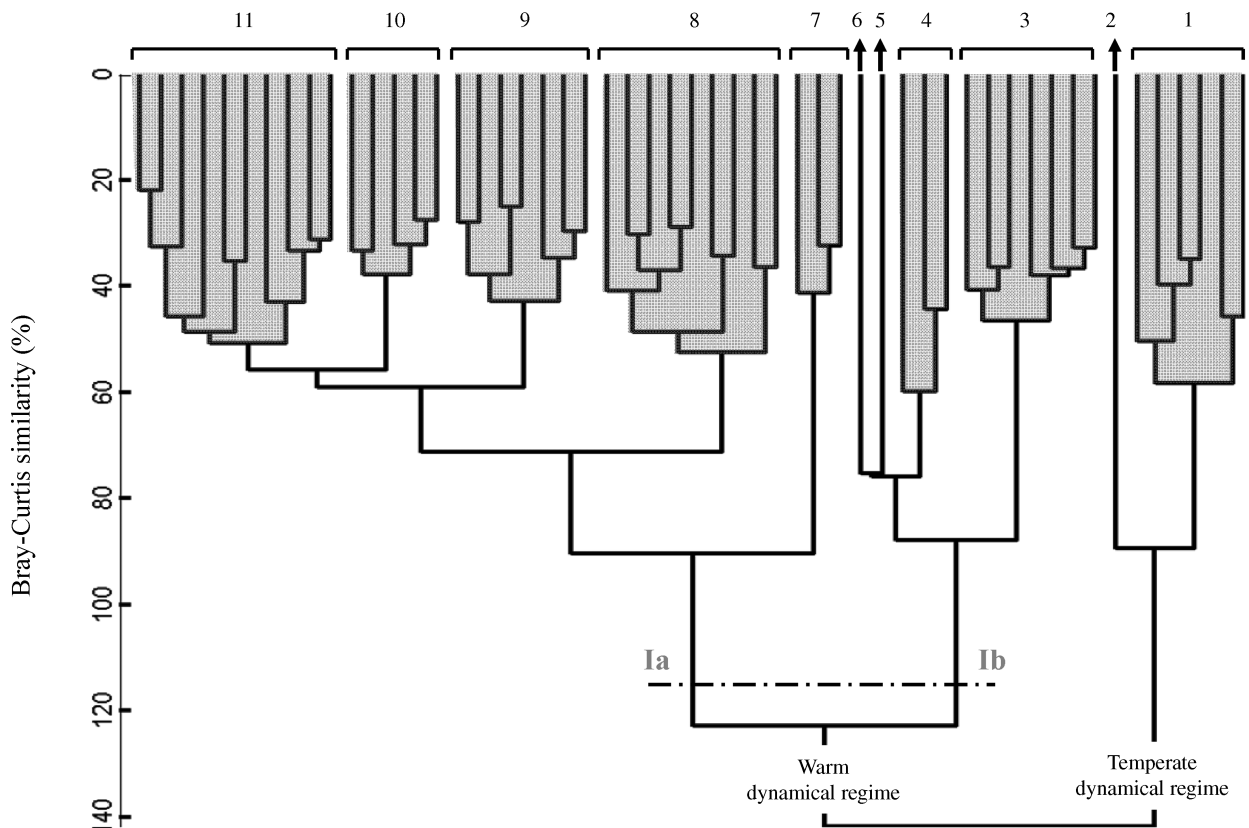


Fig. 2. Dendrogram from the cluster analysis performed on a Bray–Curtis similarity matrix, using the strategy of flexible links (see method section), with all 192 calanoid copepod species recorded for the samplings carried out at the four studied sites (Pa-Li, National Power Plant, South China Sea and Peng-Hu island) around Taiwan as variables. The calanoid copepod assemblages, identified at various levels of resolution (from the 3rd to the 10th level), are numbered and tinted in grey. The newly obtained group at the second hierarchical level is shown by discontinuous lines and is labelled.

temperature (Fig. 3) and seasonal variation of the average 20-m depth current (Fig. 4).

The analysis of the different clusters, based on all these characteristics, revealed distinct patterns in the calanoid assemblages that are presented below.

Structure 1: early northeasterly monsoon community in subtropical waters

The first assemblage displayed its presence principally in winter and was characterized by temperate water temperature ($20^{\circ}\text{C} \pm 2.5^{\circ}\text{C}$, Table II and III). Its four indicator species: *Paracalanus parvus*, *Scolecithricella longispinosa*, *Euchaeta concinna* and *S. abyssalis* exhibited IndVal values of 71, 65, 58 and 33, respectively (Table III). The seasonal scale associated with this group corresponded to the period when the northeasterly monsoon prevails. The SST map for January 2004 shows the effect of the monsoon on the water dynamics with a cool water intrusion from the north along the Chinese coast (Fig. 3A). This created a particular west–east gradient of temperature in the northern Taiwan Strait and

blocked the warm water intrusion from the south. In both northern sampling areas, the water temperature reached nearly 20°C (Fig. 3A).

Structure 2: cold water mass from East China Sea

Cluster 2 was identified rapidly (Fig. 2) and corresponded to a northwestern calanoid community from a cold water mass ($14^{\circ}\text{C} \pm 0.02^{\circ}\text{C}$) (Tables II and III). The two main indicators of this assemblage (Table III) presented different ecological niches since *P. aculeatus* is a warm-water species whereas *Calanus sinicus* is a cold-temperate species. The co-occurrence of these species in this assemblage was confirmed by the particular presence of two different water masses during March 2000 on the sea surface temperature map (Fig. 3A). This map shows the mark left by a previous and peculiar intrusion, during winter, of a cool water mass (around 17°C) in the northwestern part of the Taiwan Strait. In the eastern part of the Taiwan Strait, a warmer water mass (around 23°C) was observed (Fig. 3A). This warmer water mass could have been introduced by the

Table III: Indicator species, mean temperature and its SD associated with 11 identified assemblages obtained at various hierarchical levels (from the 3rd to the 10th level)

Cluster	Label	Species (IndVal)	Mean T °C	Nb.
1	A4_1	<i>Parac. parv.</i> (71); <i>Eucha. conc.</i> (58); <i>Scole. longi.</i> (65); <i>Scole.abys.</i> (33)	20 (±2.5)	6
2	A4_2	<i>Parac. acule.</i> (98); <i>Calan. sinic.</i> (75)	14 (#)	1
3	A5_2	<i>Pleur. grac.</i> (97); <i>Labid. detru.</i> (94); <i>Centro. calan.</i> (81); <i>Neoca. grac.</i> (80); <i>Nanno. minor.</i> (77); <i>Parac. trunc.</i> (74); <i>Claus. arcui.</i> (74); <i>Pleur. abdom.</i> (71); <i>Ponte. pluma.</i> (70); <i>Claus. masti.</i> (70); <i>Acroc. monac.</i> (69); <i>Canda. ethio.</i> (69); <i>Scole. danae.</i> (67); <i>Canda. catul.</i> (65); <i>Claus. furca.</i> (58); <i>Caloc. plumu.</i> (55); <i>Centro. grac.</i> (52); <i>Calan. minor.</i> (44); <i>Pareu. atten.</i> (43); <i>Subeu. subcr.</i> (42); <i>Cosmo. darwi.</i> (41); <i>Eucha. rima.</i> (41); <i>Acroc. grac.</i> (39); <i>Labid. acuta.</i> (35); <i>Caloc. pavo.</i> (33); <i>Temor. turbi.</i> (31); <i>Canda. pachy.</i> (31); <i>Eucha. indic.</i> (31); <i>Ponte. fera.</i> (30); <i>Caloc. grac.</i> (29); <i>Pleur. robus.</i> (29); <i>Labid. minut.</i> (29); <i>Parac. nudus.</i> (28); <i>Canda. brady.</i> (27)	27.9 (±1.2)	7
4	A6_2	<i>Undin. vulga.</i> (52); <i>Acroc. grac.</i> (51)	27.3 (±2.5)	3
5	A7_2	<i>Subeu. pilea.</i> (100); <i>Centr. s. inen.</i> (100); <i>Rhinc. nasut.</i> (96); <i>Acart. pacif.</i> (90); <i>Ponte. regal.</i> (72); <i>Parae. russe.</i> (66); <i>Eucha. indic.</i> (65); <i>Canda. pachy.</i> (59); <i>Labid. kroey.</i> (58); <i>Calan. minor.</i> (58); <i>Temor. disca.</i> (39); <i>Calan. carin.</i> (33); <i>Scole. longi.</i> (29)	23.6 (#)	1
6	A7_1	<i>Halop. longi.</i> (100); <i>Centr. tenui.</i> (98); <i>Mecyn. claus.</i> (98); <i>Lucic. flavi.</i> (95); <i>Subeu. subte.</i> (71); <i>Claus. furca.</i> (57); <i>Acroc. monac.</i> (53); <i>Temor. disca.</i> (34); <i>Acart. negli.</i> (26)	29.4 (#)	1
7	A3_2	<i>Accro. gibbe.</i> (96); <i>Temor. turbi.</i> (81); <i>Labid. eucha.</i> (84); <i>Acart. negli.</i> (76); <i>Calano. ellip.</i> (68); <i>Parvo. crass.</i> (67); <i>Ponte. tenui.</i> (59); <i>Centro. orsin.</i> (55); <i>Cosmo. darwi.</i> (53); <i>Cantho. paupe.</i> (42); <i>Centro. furca.</i> (33)	28.5 (±1.5)	3
8	A8_2	<i>Canda. brady.</i> (64); <i>Eucha. plana.</i> (48); <i>Eucha. conc.</i> (45); <i>Acart. spini.</i> (44); <i>Centr. furca.</i> (30); <i>Subeu. crass.</i> (30)	22.5 (±2.2)	9
9	A10_2	<i>Labid. acuta.</i> (52); <i>Labid. minut.</i> (43); <i>Eucha. rima.</i> (40); <i>Subeu. crass.</i> (34); <i>Labid. eucha.</i> (31)	22.7 (±2)	7
10	A12_2	<i>Temor. turbi.</i> (28)	23.3 (±3.1)	5
11	A12_1	<i>Centr. orsin.</i> (36); <i>Parac. nanus.</i> (30); <i>Acart. eryth.</i> (28)	27.1 (±1.7)	10

The IndVal is specified for each indicator species in parentheses. Species codes (abbreviations) are shown in Table IV. The number of data considered for the SD calculation is given in parentheses.

Kuroshio branch current (KBC), when the northeastern monsoon waned in spring (Fig. 4A). The sea surface temperature map does not show clearly the intrusion of this high-temperature water mass up to the northern part of the Taiwan Strait. However, according to the mapping method and the surface current map (Fig. 4A), it could not be ruled out that this water mass reached the Pa-Li area during March 2000.

Structure 3: tropical water assemblage

The calanoid community of Peng-Hu archipelagos regrouped with most of those from the South China Sea exhibited a huge number (35) of indicator species (Table III). They represented 13 calanoid families among which the Pontelliidae and the Candaciidae were the most represented, followed by the Calanidae, the Clausocalanidae, the Paracalanidae and the Calocalanidae. The species having higher IndVal value were *Pleuromamma gracilis*, *Labidocera detruncata*, *Centropages calaninus*, *Neocalanus gracilis* with respective IndVal values of 97%, 94%, 81% and 80% (Table III). The value of water temperature associated with this cluster (28°C) was in accordance with the temperature observed in this region during summer (Fig. 3C). Although the South China Sea current pattern was rather complex in summer, the interaction with Peng-Hu could clearly be observed. The surface current, under the influence of the southwesterly monsoon, flowed northwards from

the northern part of the South China Sea through the Peng-Hu channel and on to the west of the Archipelago.

Structure 4: 2001 South China Sea community

The group of cruises carried out in SCS during 2001 was characterized by two indicator species: *Undimula vulgaris* and *Acrocalanus gracilis* with respective IndVal values of 52% and 51% (Table III). The associated averaged water temperature obtained via the cluster analysis was around 27°C (Table III). The values observed during June 2001 from the satellite image (Fig. 3D) were slightly higher (28–30°C). A west–east gradient was observed at that time due to the intrusion of a warmer water mass (30°C) from the Luzon Strait (Fig. 3D).

Structure 5: particular spring community in the north of Taiwan

The seventh hierarchical level was marked by the distinction of one particular community sampled in the NPP coastal area in May 2002 (Table II). This assemblage exhibited an average temperature linked to it of around 24°C (Table III). This subtropical spring calanoid community showed many indicator species representing nine calanoid families including Pontelliidae, Eucalanidae and Euchaetidae to quote the most important. The maximum IndVal species were

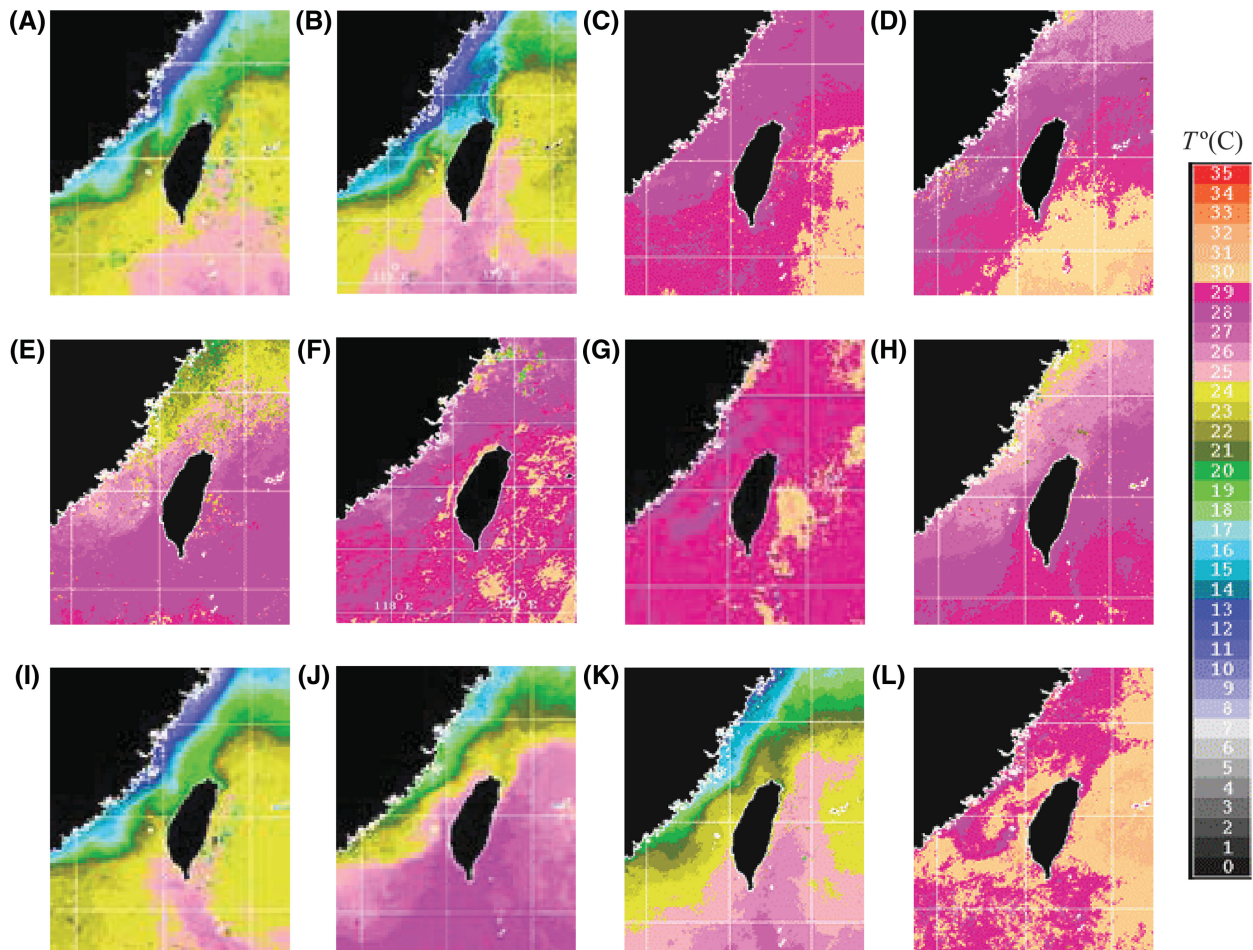


Fig. 3. Monthly average sea surface temperature derived from AVHRR for the sampling date associated with nine of the clusters studied. (A) January 2004; (B) March 2000; (C) September 2002; (D) June 2001; (E) May 2002; (F) July 1999; (G) September 2003; (H) October 2002; (I) January 2003; (J) April 2003; (K) March 2002; (L) August 2001.

Subeucalanus pileatus, *Centropages sinensis*, *Rhincalanus nasutus* and *Acartia pacifica* which exhibited the respective values of 100, 100, 96 and 90 (Table III). The sea surface temperature map of the sampling month (Fig. 3E) was in accordance with the one associated with the cluster (Table III). It revealed the presence of a warm water mass, around 24–25°C, in northern Taiwan, at a period that corresponded to the beginning of the 2002 southwesterly monsoon. Moreover, the counter-clockwise current observed in summer in this area (Fig. 4B) could be also seen on the SST map (Fig. 3E).

Structure 6: July 1999 community in SCS

One sampling of the southern tropical waters of Taiwan was separated from the other exhibiting a high water temperature of 29°C. Similar values of temperature were observed from the satellite image. The SST map

(Fig. 3F) corresponding to this sampling, exhibited the classical pattern of sea surface temperature around Taiwan when the southwesterly monsoon prevails with temperatures between 27°C and 30°C (Fig. 4). The nine indicator species of this cluster had IndVal values that spread between 100 and 26 and were representative of the eight main calanoid families.

Structure 7: warm water community in Northern Taiwan

Cluster 7 regrouped two summer sampling cruises and one in September from Pa-Li. When the Southwestern monsoon prevailed, in June–July, Pa-Li’s environment was characterized by northwestern hydrodynamic movement (Fig. 4B). This movement induced a warming of the sea surface temperature in the eastern part of the Taiwan Strait which reached around 27°C (Fig. 3D). The September cruise was associated with the end of the southwesterly monsoon in 2003. That year, the

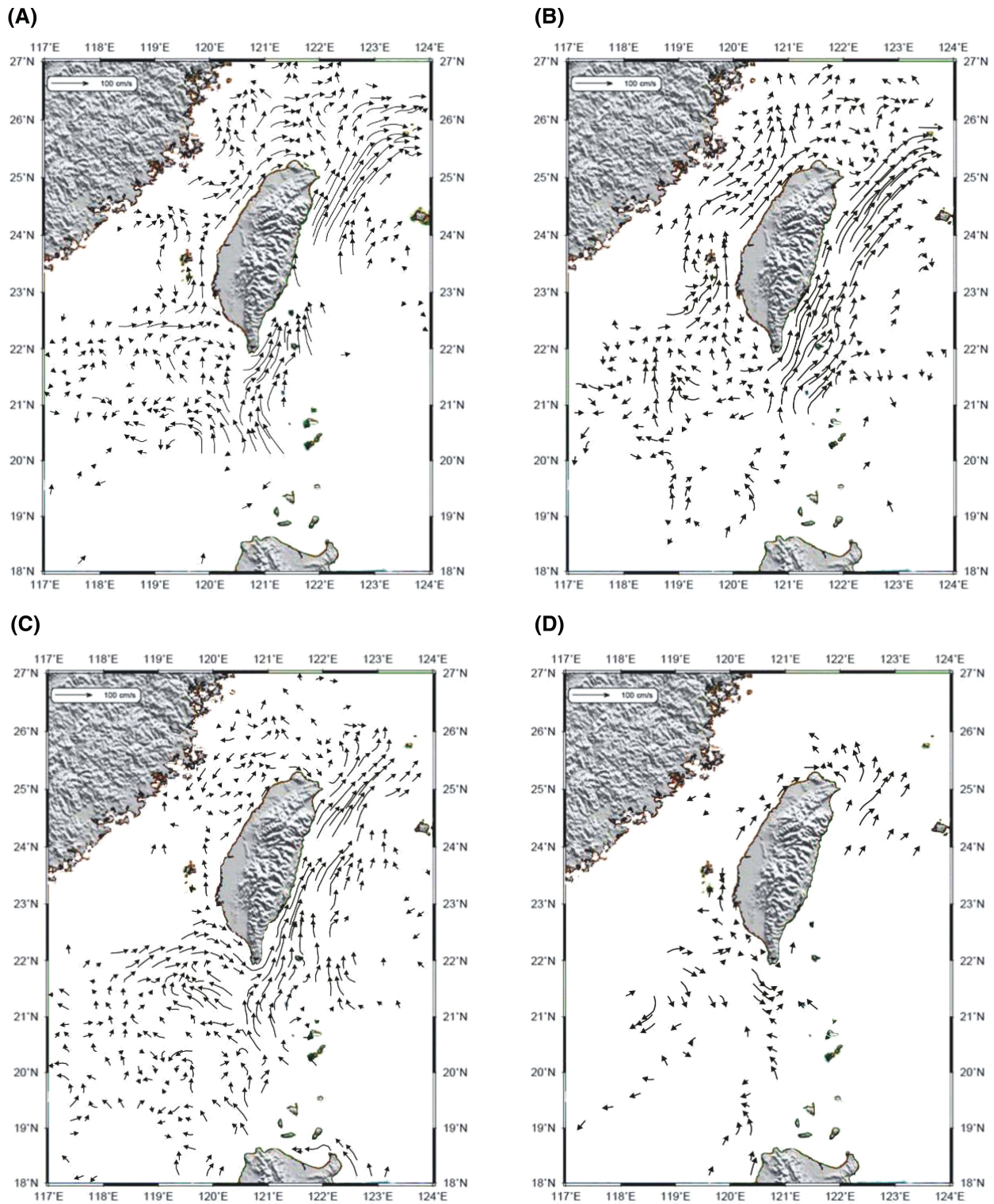


Fig. 4. Composite current velocity vector at 20-m depth for the different seasons: (A) spring (March–May), (B) summer (June–August), (C) autumn (September–November) and (D) winter (December–February). The lack of current data in the winter season resulted primarily from rough sea conditions prohibiting research vessel activities. Figure modified from NCOR Ocean Data Base (www.ncor.ntu.edu.tw).

Table IV. Faunistic list and abbreviation of all calanoid species identified over all samplings off Taiwan analysed in this study

Species name	Abbreviation	Species name	Abbreviation	Species name	Abbreviation
Acartiidae		Calanidae		Centropagidae	
<i>Acartia omori</i>	<i>Acart. omori.</i>	<i>Calanidae</i> copepodid	<i>Calan. copep.</i>	<i>Centropages copepodid</i>	<i>Centr. copep.</i>
<i>Acartia pacifica</i>	<i>Acart. pacif.</i>	<i>Calanoides carinatus</i>	<i>Calan. carin.</i>	<i>Centropages calaninus</i>	<i>Centr. calan.</i>
<i>Acartia spinicauda</i>	<i>Acart. spini.</i>	<i>Calanus sinicus</i>	<i>Calan. sinic.</i>	<i>Centropages elongatus</i>	<i>Centr. elong.</i>
<i>Acartia danae</i>	<i>Acart. danae.</i>	<i>Calanus jashnovi</i>	<i>Calan. jashn.</i>	<i>Centropages furcatus</i>	<i>Centr. furca.</i>
<i>Acartia negligens</i>	<i>Acart. negli.</i>	<i>Canthocalanus pauper</i>	<i>Canth. paupe.</i>	<i>Centropages gracilis</i>	<i>Centr. graci.</i>
<i>Acartia erythraea</i>	<i>Acart. eryth.</i>	<i>Cosmocalanus darwini</i>	<i>Cosmo. darwi.</i>	<i>Centropages pergens</i>	<i>Centr. perge.</i>
<i>Acartia</i> sp.	<i>Acart. sp.</i>	<i>Mesocalanus tenuicornis</i>	<i>Mesoc. tenui.</i>	<i>Centropages orsini</i>	<i>Centr. orsin.</i>
		<i>Nannocalanus minor</i>	<i>Nanno. minor.</i>	<i>Centropages sinensis</i>	<i>Centr. sinen.</i>
		<i>Neocalanus gracilis</i>	<i>Neoca. graci.</i>	<i>Centropages tenuiremis</i>	<i>Centr. tenui.</i>
		<i>Neocalanus robustior</i>	<i>Neoca. robus.</i>		
		<i>Undinula vulgaris</i>	<i>Undin. vulga.</i>	Clausocalanidae	
Aetideidae		Calocalanidae		<i>Clausocalanus</i> sp.	<i>Claus. sp.</i>
<i>Aetideopsis</i> sp	<i>Aetid. sp.</i>	<i>Calocalanus contractus</i>	<i>Caloc. contr.</i>	<i>Clausocalanus arcuicornis</i>	<i>Claus. arcui.</i>
<i>Aetideus acutus</i>	<i>Aetid. acutu.</i>	<i>Calocalanus gracilis</i>	<i>Caloc. graci.</i>	<i>Clausocalanus farrani</i>	<i>Claus. farra.</i>
<i>Aetideus giesbrechti</i>	<i>Aetid. giesb.</i>	<i>Calocalanus pavo</i>	<i>Caloc. pavo.</i>	<i>Clausocalanus furcatus</i>	<i>Claus. furca.</i>
<i>Chirundina streetsii</i>	<i>Chiru. stree.</i>	<i>Calocalanus pavoninus</i>	<i>Caloc. pavon.</i>	<i>Clausocalanus mastigophorus</i>	<i>Claus. masti.</i>
<i>Euchirella amoena</i>	<i>Euchi. amoen.</i>	<i>Calocalanus plumulosus</i>	<i>Caloc. plumu.</i>	<i>Clausocalanus minor</i>	<i>Claus. minor.</i>
<i>Euchirella curticauda</i>	<i>Euchi. curt.</i>	<i>Calocalanus</i> sp.	<i>Caloc. sp.</i>	<i>Clausocalanus lividus</i>	<i>Claus. livid.</i>
<i>Euchirella indica</i>	<i>Euchi. indic.</i>	<i>Calocalanus</i> spp.	<i>Caloc. spp.</i>	<i>Clausocalanus pergens</i>	<i>Claus. perge.</i>
<i>Euchirella galeata</i>	<i>Euchi. galea.</i>	<i>Calocalanus styliremis</i>	<i>Caloc. styli.</i>	<i>Clausocalanus</i> spp.	<i>Claus. spp.</i>
<i>Euchirella pulchra</i>	<i>Euchi. pulch.</i>			Eucalanidae	
<i>Euchirella</i> sp.	<i>Euchi. sp.</i>			<i>Eucalanidae</i> copepodid	<i>Eucal. copep.</i>
<i>Euchirella venusta</i>	<i>Euchi. venus.</i>			<i>Eucalanus elongatus</i>	<i>Eucal. elong.</i>
<i>Undeuchaeta major</i>	<i>Undeu. major.</i>			<i>Pareucalanus attenuatus</i>	<i>Pareu. atten.</i>
<i>Undeuchaeta plumosa</i>	<i>Undeu. plumo.</i>			<i>Paraeucalanus langae</i>	<i>Parae. langa.</i>
				<i>Rhincalanus nasutus</i>	<i>Rhinc. nasut.</i>
				<i>Rhincalanus rostrifrons</i>	<i>Rhinc. rostr.</i>
				<i>Subeucalanus crassus</i>	<i>Subeu. crass.</i>
				<i>Subeucalanus mucronatus</i>	<i>Subeu. mucro.</i>
				<i>Subeucalanus pileatus</i>	<i>Subeu. pilea.</i>
				<i>Subeucalanus subcrassus</i>	<i>Subeu. subcr.</i>
				<i>Subeucalanus subtenuis</i>	<i>Subeu. subte.</i>
Arietellidae		Candaciidae			
<i>Arietellus simplex</i>	<i>Ariet. simpl.</i>	<i>Candaciidae</i> copepodid	<i>Canda. copep.</i>		
<i>Metacalanus aurivilli</i>	<i>Metac. auriv.</i>	<i>Candacia bipinnata</i>	<i>Canda. bipin.</i>		
<i>Metacalanus</i> sp.	<i>Metac. sp.</i>	<i>Candacia bradyi</i>	<i>Canda. brady.</i>		
<i>Arietellidae</i> sp	<i>Ariet. sp.</i>	<i>Candacia catula</i>	<i>Canda. catul.</i>		
		<i>Candacia curta</i>	<i>Canda. curta.</i>		
		<i>Candacia discaudata</i>	<i>Canda. disca.</i>		
		<i>Candacia ethiopica</i>	<i>Canda. ethio.</i>		
		<i>Candacia guggenheimi</i>	<i>Canda. gugge.</i>		
		<i>Candacia larva</i>	<i>Canda. larva.</i>		
		<i>Candacia longimana</i>	<i>Canda. longi.</i>		
		<i>Candacia pachydactyla</i>	<i>Canda. pachy.</i>		
		<i>Candacia</i> spp.	<i>Canda. spp.</i>		
		<i>Paracandacia bispinosa</i>	<i>Parac. bispi.</i>		
		<i>Paracandacia simplex</i>	<i>Parac. simpl.</i>		
		<i>Paracandacia truncata</i>	<i>Parac. trunc.</i>		
Augaptilidae		Paracalanidae		Pseudodiaptomidae	
<i>Augaptilus longicaudatus</i>	<i>Augap. longi.</i>	<i>Acrocalanus</i> sp	<i>Acroc. sp.</i>	<i>Pseudodiaptomus annandalei</i>	<i>Pseud. annan.</i>
<i>Euaugaptilus elongatus</i>	<i>Euaug. elong.</i>	<i>Acrocalanus</i> sp1	<i>Acroc. sp1.</i>	Scolecithricidae	
<i>Euaugaptilus hecticus</i>	<i>Euaug. hecti.</i>	<i>Acrocalanus longicornis</i>	<i>Acroc. longi.</i>	<i>Scolecithricidae</i> copepodid	<i>Scole. copep.</i>
<i>Euaugaptilus nodifrons</i>	<i>Euaug. nodif.</i>	<i>Acrocalanus gibber</i>	<i>Acroc. gibbe.</i>	<i>Lophothrix</i> sp.	<i>Lopho. sp.</i>
<i>Haloptilus acutifrons</i>	<i>Halop. acuti.</i>	<i>Acrocalanus gracilis</i>	<i>Acroc. graci.</i>	<i>Scaphocalanus brevicornis</i>	<i>Scaph. brevi.</i>
<i>Haloptilus austini</i>	<i>Halop. austi.</i>	<i>Acrocalanus indicus</i>	<i>Acroc. indic.</i>	<i>Scolecithricella abyssalis</i>	<i>Scole. abyss.</i>
<i>Haloptilus longicornis</i>	<i>Halop. longi.</i>	<i>Acrocalanus monachus</i>	<i>Acroc. monac.</i>	<i>Scolecithricella dentata</i>	<i>Scole. denta.</i>
<i>Haloptilus mucronatus</i>	<i>Halop. mucro.</i>	<i>Paracalanus aculeatus</i>	<i>Parac. acule.</i>	<i>Scolecithricella emarginata</i>	<i>Scole. emarg.</i>
<i>Haloptilus ornatus</i>	<i>Halop. ornat.</i>	<i>Paracalanus gracilis</i>	<i>Parac. graci.</i>	<i>Scolecithricella longispinosa</i>	<i>Scole. longi.</i>
<i>Haloptilus oxycephalus</i>	<i>Halop. oxyce.</i>	<i>Paracalanus nanus</i>	<i>Parac. nanus.</i>	<i>Scolecithricella minor</i>	<i>Scole. minor.</i>
<i>Haloptilus paralongicirrus</i>	<i>Halop. paral.</i>	<i>Paracalanus nudus</i>	<i>Parac. nudus.</i>	<i>Scolecithricella minor</i>	<i>Scole. minor.</i>
<i>Haloptilus spiniceps</i>	<i>Halop. spini.</i>	<i>Paracalanus parvus</i>	<i>Parac. parvu.</i>	<i>Scolecithricella tenuiserrata</i>	<i>Scole. tenui.</i>
Euchaetidae		<i>Paracalanus serrulus</i>	<i>Parac. serru.</i>	<i>Scolecithricella vittata</i>	<i>Scole. vitta.</i>
<i>Euchaetidae</i> copepodid	<i>Eucha. copep.</i>	<i>Paracalanus</i> sp.	<i>Parac. sp.</i>	<i>Scolecithricella</i> spp.	<i>Scole. spp.</i>
<i>Euchaeta concinna</i>	<i>Eucha. conci.</i>	<i>Paracalanus</i> spp.	<i>Parac. spp.</i>	<i>Scolecithrix bradyi</i>	<i>Scole. brady.</i>
<i>Euchaeta indica</i>	<i>Eucha. indic.</i>	<i>Parvocalanus crassirostris</i>	<i>Parvo. crass.</i>	<i>Scolecithrix danae</i>	<i>Scole. danae.</i>
<i>Euchaeta longicornis</i>	<i>Eucha. longi.</i>			<i>Scolecithrix nicobarica</i>	<i>Scole. nicob.</i>
<i>Euchaeta media</i>	<i>Eucha. media.</i>			<i>Scottocalanus</i> sp.	<i>Scott. sp.</i>
<i>Euchaeta plana</i>	<i>Eucha. plana.</i>			<i>Scottocalanus securifrons</i>	<i>Scott. secur.</i>
<i>Euchaeta rimana</i>	<i>Eucha. riman.</i>				
<i>Euchaeta</i> sp.	<i>Eucha. sp.</i>				
<i>Paraeuchaeta russelli</i>	<i>Parae. russe.</i>				
<i>Paraeuchaeta</i> copepodid	<i>Parae. copep.</i>				
Heterorhabdidae		Phaennidae			
<i>Heterorhabdidae</i> copepodid	<i>Heter. copep.</i>	<i>Phaenna spinifera</i>	<i>Phaen. spini.</i>		
<i>Heterorhabdus abyssalis</i>	<i>Heter. abyss.</i>				
<i>Heterorhabdus papilliger</i>	<i>Heter. papil.</i>				
<i>Heterorhabdus spinifrons</i>	<i>Heter. spini.</i>				
<i>Heterorhabdus spinosus</i>	<i>Heter. spino.</i>				
<i>Heterorhabdus subspinifrons</i>	<i>Heter. subsp.</i>				
<i>Paraheterorhabdus vipera</i>	<i>Parah. viper.</i>				

(continued)

Table IV: Continued

Lucicutiidae		Pontellidae		Spinocalanidae	
<i>Lucicutia clausi</i>	<i>Lucic. claus.</i>	<i>Pontellidae</i> copepodid	<i>Ponte. copep.</i>	<i>Monacilla gracillis</i>	<i>Monac. graci.</i>
<i>Lucicutia curta</i>	<i>Lucic. curta.</i>	<i>Calanopia elliptica</i>	<i>Calan. ellip.</i>		
<i>Lucicutia flavicornis</i>	<i>Lucic. flavi.</i>	<i>Calanopia minor</i>	<i>Calan. minor.</i>	Temoridae	
<i>Lucicutia gausssae</i>	<i>Lucic. gaus.</i>	<i>Labidocera acuta</i>	<i>Labid. acuta.</i>	<i>Temora discaudata</i>	<i>Temor. disca.</i>
<i>Lucicutia gemina</i>	<i>Lucic. gemin.</i>	<i>Labidocera bipinnata</i>	<i>Labid. bipin.</i>	<i>Temora stylifera</i>	<i>Temor. styli.</i>
<i>Lucicutia ovalis</i>	<i>Lucic. ovali.</i>	<i>Labidocera detruncata</i>	<i>Labid. detru.</i>	<i>Temora turbinata</i>	<i>Temor. turbi.</i>
<i>Lucicutia sp.</i>	<i>Lucic. sp..</i>	<i>Labidocera euchaeta</i>	<i>Labid. eucha.</i>	<i>Tomoropia mayumbaensis</i>	<i>Tomor. mayum.</i>
		<i>Labidocera kroeyeri</i>	<i>Labid. kroey.</i>		
Mecynoceridae		<i>Labidocera minuta</i>	<i>Labid. minut.</i>	Tortanidae	
<i>Mecynocera clausi</i>	<i>Mecyn. claus.</i>	<i>Labidocera pavo</i>	<i>Labid. pavo.</i>	<i>Tortanus</i>	<i>Tortan. graci.</i>
		<i>Pontella chierchiaie</i>	<i>Ponte. chier.</i>	(<i>Tortanus</i>) <i>gracilis</i>	
Metridinidae		<i>Pontella danae</i>	<i>Ponte. danae.</i>		
<i>Pleuromamma copepodid</i>	<i>Pleur. copep.</i>	<i>Pontella fera</i>	<i>Ponte. fera.</i>		
<i>Pleuromamma abdominalis</i>	<i>Pleur. abdom.</i>	<i>Pontellina morii</i>	<i>Ponte. morii.</i>		
<i>Pleuromamma gracilis</i>	<i>Pleur. graci.</i>	<i>Pontella securifer</i>	<i>Ponte. secur.</i>		
<i>Pleuromamma robusta</i>	<i>Pleur. robus.</i>	<i>Pontella sinica</i>	<i>Ponte. sinic.</i>		
<i>Pleuromamma xiphias</i>	<i>Pleur. xiphi.</i>	<i>Pontellina plumata</i>	<i>Ponte. pluma.</i>		
		<i>Pontellopsis regalis</i>	<i>Ponte. regal.</i>		
		<i>Pontellopsis strenua</i>	<i>Ponte. stren.</i>		
		<i>Pontellopsis tenuicauda</i>	<i>Ponte. tenui.</i>		
		<i>Pontellopsis villosa</i>	<i>Ponte. villo.</i>		
		<i>Pontellopsis yamadai</i>	<i>Ponte. yamad.</i>		

monsoon was quite strong since even in the beginning of autumn (September), waters surrounding Taiwan had surface temperatures above 28°C (Fig. 3G). The SST maps (Fig. 3D and G) as well as the associated temperature extracted from the cluster analysis (28.5°C) confirmed a link of the assemblage to a warm dynamical regime. In its entirety, this warm water cluster presented 11 indicator species. Among them, *Acrocalanus gibber*, *Temora turbinata*, *Labidocera euchaeta* and *Acartia negligens* were identified with the respective IndVal values 96, 81, 84 and 76 (Table III). Deeper investigation (i.e. 25th hierarchical level) allowed to specify the September 2003 sampling characterized by *A. negligens*, *Cosmocalanus darwini*, *A. gibber*, *Parvocalanus crassirostris*, *L. euchaeta*, *Pontellopsis tenuicauda* and was associated with a high temperature value (i.e. 29°C).

Structure 8: autumn and winter northern community

The assemblage identified as the NE monsoon community in the northern part of Taiwan was dominated by *Candacia bradyi* and *E. concinna* (Table III). The water temperature associated with the calanoid community observed in the northern neritic area during autumn and winter was 22.5°C.

In order to characterize the water mass affiliated to this cluster, the sea surface temperature recorded during the beginning of the monsoon (October 2002) and its prevalence (January 2003) were chosen (Fig. 3H and I). During October 2002, the sea temperature around

Taiwan showed high values around 26–27°C (Fig. 3H), whereas the water temperature in January 2003 was around 19°C (Fig. 3I). The intrusion of water masses from the north could be observed from the beginning of October (Fig. 3H) to January when it finally reached Taiwan (Fig. 3I).

Structure 9: the northern NE–SW monsoon transition community

The spring assemblage A10_2 identified in the transition period between northeasterly and southwesterly monsoon (Table II) exhibited five indicator species: three of the Pontellidae family (*Labidocera acuta*, *L. minuta*, *L. eucha*), *Euchaeta rimana* and *Subeucalanus crassus* (Table III). The common sampling month for both sites, April 2003, was chosen to characterize the affiliated dynamical regime. The sea surface temperature observed during April 2003 retained the influence of both monsoon regimes. The remnant of the northeasterly monsoon could be noticed by the attendance of a cold water mass (19°C) in the northeastern part of the Taiwan Strait and a warmer water intrusion (25°C) from the South China Sea which reached the Pa-Li area (Fig. 3I). In the north, the coast to offshore gradient of temperature revealed the beginnings of the coastal remoteness of Kuroshio's main axis in early summer and the creation of the counter current which maintained cooler water (23–24°C) in the NPP sampling zone.

Structure 10: the peculiar 2002 community at northern sites
Cluster 10 was characterized by only one indicator species *T. turbinata* (Table III). The associated water temperature value was 23°C. The water dynamic properties of this group corresponded principally to the beginning of the southwesterly monsoon in 2002. On the March 2002 SST map, the southwestern movement of the China coastal current which strived the coast, bringing colder waters during NE monsoon, was still present (Fig. 3K). Moreover, the warm current coming from the Taiwan Strait began to reach the northern coast (Figs. 3K and 4). At that time, the temperature at the northern Taiwan coast started to increase with values between 20°C and 24°C (Fig. 3K).

Structure 11: southwesterly monsoon community in the north
We limited our ascending analysis to this hierarchical level and we will focus on the assemblage A12_1 characterized by three indicator species *Centropages orsini*, *Paracalanus nanus*, *Acartia erythraea* with relatively low IndVal values (36, 30 and 28, respectively). The water temperature associated with this assemblage presents a value of around 27°C (Table III).

From the satellite image, we obtained temperatures above 29°C for the entire vicinity of Taiwan during August 2001 (Fig. 3L). The SST map gave a good representation of the typical environment observed under the influence of the SW monsoon. Especially in August when the SW monsoon prevailed, the warm water from the south surrounded the island entirely.

Seasonal distribution of the target species in the northern coastal area

Following the previously obtained results, target calanoid species were assigned to each season. We thus selected *C. sinicus* for spring, *T. turbinata* for summer, *A. gibber* for autumn and *P. parvus* for winter. Figure 5 presents the seasonal distribution of each species in the northern Taiwan area during 2002.

During the year 2002, *C. sinicus* was found mainly in winter and spring (Fig. 5, A1 and D1). For both seasons, the maximum density was observed in the east part of the north Taiwan coast, representing the NPP sampling area. Highest abundances of *C. sinicus* were observed in spring with densities reaching 71.98 ind. m⁻³ but were in average more important during winter (Fig. 5). Abundance of this species remained low during summer and autumn (Fig. 5B1 and C1).

The summer season representative, *T. turbinata*, occurred throughout the year 2002 in this northern

Taiwan coastal area with lowest densities observed during winter and autumn (Fig. 5C2 and D2). Increasing densities of *T. turbinata* are observed during spring and reach, relatively speaking, an extremely high density in summer (659 ind. m⁻³ on average with a maximum value of 12 684 ind. m⁻³).

Another species was present throughout the year 2002 in this northern coastal region, *A. gibber* associated with autumn. Nevertheless, *A. gibber* is less abundant than *T. turbinata* and its distribution showed marked variation all along the year in this region. This species was maintained at low values during summer and winter (Fig. 5B3 and D3). But it was present during spring and autumn (Fig. 5A3 and C3), with higher densities (97 ind. m⁻³) in autumn. However, during this season, no individual was recorded in NPP samples (Fig. 5C3).

For the last season representative, *P. parvus*, its seasonal distribution pattern was clearly different from the other indicator species. *Paracalanus parvus* was present consistently only during spring and winter (Fig. 5A4 and D4) but in relatively low proportions compared to *C. sinicus* and *T. turbinata*. However, its highest abundances were recorded in winter when it reached an average density of 1.9 ind. m⁻³ with an observed maximum value of 9.3 ind. m⁻³.

DISCUSSION

Only a few investigations on the relation between hydrodynamics and calanoid communities have been performed in Taiwan waters (e.g. Hsieh *et al.*, 2004; Lan *et al.*, 2004; Hwang and Wong, 2005). Moreover, no comparable data set has been analysed at the scale of the current study. The area investigated with the sampling cruises taken into consideration for this study encompassed two of the three distinct but contiguous ecosystems that surround Taiwan. This study, therefore, provides a comprehensive coverage of the majority of Taiwan's oceanographic zones and an excellent data base from which to assess an association between local calanoid communities and the hydrodynamic regimes of different water masses.

For identifying assemblages in ecology, classification methods have long been used as useful tools and are often the first step in unravelling the relationship between assemblages and environmental conditions. This statistical method which allowed the characterization of calanoid assemblages in this study had already proved to be an efficient tool for the mapping of different assemblages of different organisms (Anneville *et al.*, 2002, 2004; Souissi *et al.*, 2001). Among the 11 studied calanoid copepod assemblages identified by cluster

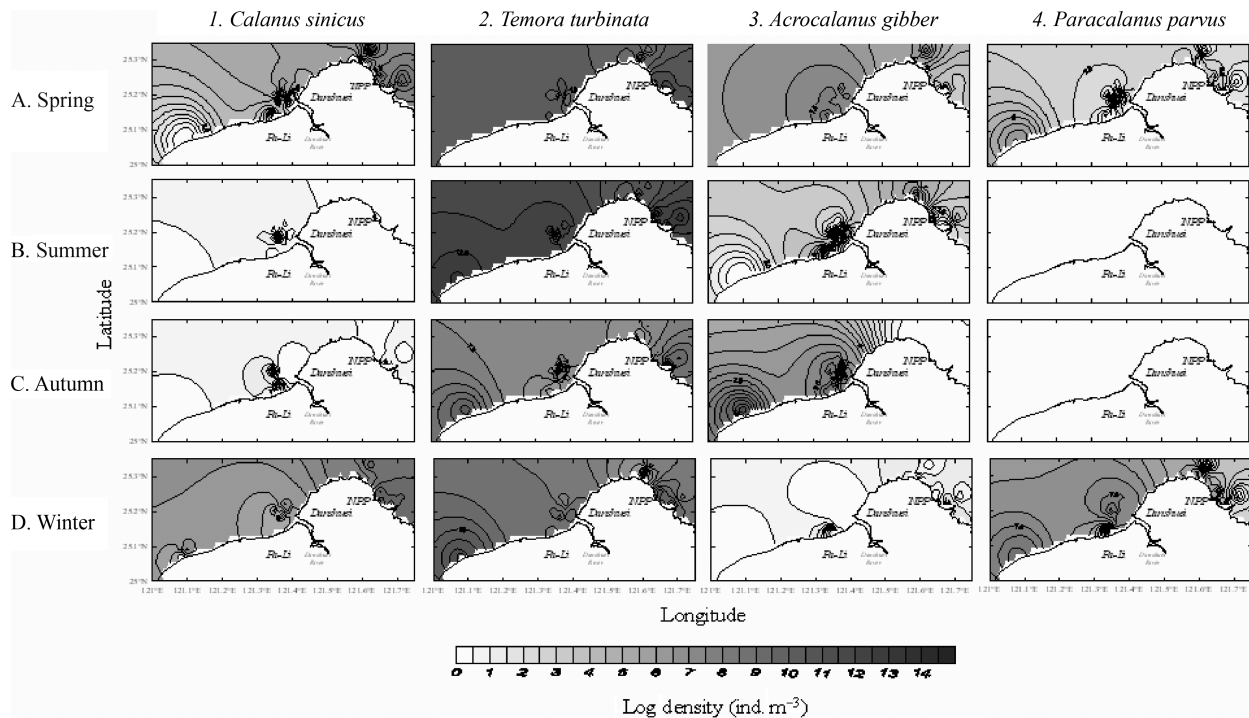


Fig. 5. Seasonal distribution and density (in $\log \text{ind.m}^{-3}$) of four target species: 1. *Calanus sinicus*, 2. *Temora turbinata*, 3. *Acrocalanus gibber* and 4. *Paracalanus aculeatus* sampled with a 333- μm mesh net in the northern coastal area in 2002. Data were averaged and girded for each season: A. spring (March-May), B. summer (June-August), C. autumn (September-November) and D. winter (December-February 2003).

analysis, two (i.e. A4_2 and A5_2) included indicator species that were defined as dominant species by previous studies, using different approaches (Hwang *et al.*, 1998; 2004a, 2006; Wong *et al.*, 1998; Hsiao *et al.*, 2004; Lo *et al.*, 2004b). The distinct assemblage linked with the spring hydrodynamic regime in the northwest of Taiwan is a typical feature of the northern part of the Taiwan Strait, as found in previous studies. For example, samples from the entire Taiwan Strait by Hsieh *et al.* (Hsieh *et al.*, 2004) revealed *C. sinicus* and *P. aculeatus* as indicator species of the China Coastal Waters and Kuroshio Branch Waters. The extracted assemblage found to encompass the cruise carried out in Peng-Hu (A5_2) was identified by species including *L. detrunata*, *C. calaninus*, *Nannocalanus minor* and *Clausocalanus arcuicornis* supporting the observation made by Lo *et al.* (Lo *et al.*, 2004b) concerning the 20 most abundant species. Besides these similar results, our study presented eight copepod assemblages that have, as far as we know, never been mentioned so far. During the examination of these assemblages, the characteristics of the indicator species of each cluster were found to match fairly well with the hydrodynamic regimes.

The results obtained also confirmed the generally held assumption that temporal changes in ecosystems can be described as regular processes (Frontier and

Pichod Viale, 1991) with some sudden transitions depending on the kind and intensity of disturbances (Petraitis and Latham, 1999). When the disturbances are smooth, communities blend gradually into another, so that they overlap in a continuum and there are no sharply defined boundaries.

Taiwan coastal waters are strongly disturbed because of the influence of several major ocean currents and water masses, themselves strongly influenced by monsoon systems (Wong *et al.*, 2000; Jan *et al.*, 2002; Lee and Chao, 2003; Liu *et al.*, 2003; Tseng and Shen, 2003; Hwang *et al.*, 2004b, 2006; Hwang and Wong, 2005). As a consequence, the previously mentioned continuum can thus be seen as a succession of different calanoid communities throughout the year.

Succession of different calanoid communities linked with hydrodynamics

As the hydrodynamics are strongly affected by monsoons (Wyrtki, 1961), we will define the beginning of our succession when the southwesterly monsoon increases (i.e. in June). The indicator species of the summer community in the northern area is the neritic species *T. turbinata* which occurred all year in northern

coastal waters of Taiwan, with higher abundances during summer (Fig. 5).

As it has been observed in New Zealand (Bradford, 1997), the quantitative distribution of *T. turbinata* in summer appears to be governed by subtropical currents and by its nutritional requirements. The area where this summer assemblage occurs, corresponds to the coastal waters off the Danshuei River estuary (named Pa-Li in this work), where the intrusion of South China Sea Coastal Waters driven by the south-westerly monsoon brings warm waters (Jan *et al.*, 1995). During summer, South China Sea surface waters intrude into the Taiwan Strait and pass northwards through the Peng-Hu Channel (Fig. 4B). Fang and Yu (Fang and Yu, 1981) already observed this intrusion in the Peng-Hu channel during summer. This is supported by the presence of indicator species, such as the warm-water species *A. gracilis* for the two tropical assemblages (A5_2 and A6_2) (Takahashi and Hirakawa, 2001). *Acrocalanus gracilis* is the most dominant copepod in the northern South China Sea (Hwang *et al.*, 2000a). Moreover, among the indicator species of the cluster that gathered the sampling from Peng-Hu with some from SCS, *L. detruncata*, *C. calaninus*, *Acrocalanus monachus* are all tropical species common in the Taiwan Strait, that show a higher abundance in summer (Chen and Zhang, 1965; Lo *et al.*, 2004b). The presence of these species within the Peng-Hu island summer community can therefore be related to this intrusion of warm water from the south throughout the Peng-Hu channel due to the influence of the southwesterly monsoon.

During the SW monsoon, the water temperature of Taiwan coastal waters is comparatively high and a new community appears in the northern part of the Taiwan Strait. This summer community, indicated by *T. turbinata*, is characterized by a mixing of local tropical neritic species from the north and the south of the Taiwan Strait. *Acrocalanus gibber* (Hsieh *et al.*, 2004; Lan *et al.*, 2004) and *L. euchaeta*, showing population increases with increasing temperature in Xiamen Harbor (Lin and Li, 1991), are originated from the north. Among the species from the south, *P. crassirostris* exhibits a higher abundance during autumn in Tapon Bay, southwestern Taiwan. *Acartia negligens* represents this assemblage as well, but is considered as an oceanic species. The co-occurrence of coastal and oceanic species is in agreement with the abundance of those species in their area of origin and the current pattern in autumn (Fig. 4C). Northern species that were abundant in winter were brought down from the north of Taiwan by the China Coastal current, whereas the warm branch of the Kuroshio flowing northward, along the eastern part

of the Taiwan Strait, introduces more southern species. At the northeastern coast, the main streaming of the Kuroshio makes its contribution by bringing some oceanic species to the north.

From October to January, Taiwan waters are the subject of strong and rapid modifications. The sea surface temperature, being most influential of the north-easterly monsoon initially in October, presents a completely different pattern. From the beginning of the NE monsoon (i.e. October) until February, the colder water masses from the north are transported along the mainland China coast, creating a west-east temperature gradient. This gradual influence is indicated by the presence of two calanoid communities at the northern coast of Taiwan. For the cluster that encompassed principally the samplings carried out in Pali (A4_1), three indicator species *E. concinna*, *P. parvus* and *S. longispinosus*, are commonly found in the coastal waters of China.

The cluster analysis provided another calanoid assemblage (A8_2) for the same period (i.e. September–January) but related principally to sampling areas in the northeast of Taiwan. This community is represented by species from coast of mainland China. Their presence can be linked with colder water masses from the north (Fig. 4C), since *Acartia spinicauda*, for example, is a common species in coastal areas of the Zhejiang province of mainland China, northwest of Taiwan. The widely spread species *E. concinna*, commonly observed in coastal waters of China provides another example. The tropical oceanic *C. bradyi* was identified as an indicator species of this calanoid community, suggesting its association with the influence of the Kuroshio intrusion in the area north of Taiwan during winter (Fig. 4D). Hsieh *et al.* (Hsieh *et al.*, 2005) gaining similar results with the warm water species *Pseudocalanus furcatus* concluded that this hydrodynamic condition forms a seasonal eddy that accommodated warm-water species. This result emphasizes that, although the two northern sampling areas are linked and interact with each other via strong current activities, the calanoid copepod composition in each area appears to be controlled by local water mass dynamics as well.

Finally, the transition phase between the two monsoons in spring provides conditions for the appearance of a particular calanoid copepod community. Knowledge of the Taiwan Strait circulation (Jan *et al.*, 2002) and previous studies on copepods in coastal waters of the northwestern part of Taiwan (Hsieh *et al.*, 2004, 2005; Lan *et al.*, 2004; Hwang *et al.*, 2006) indicates that the structure of copepod communities during spring would be due to the waning of the NE monsoon. This decrease of strength allows the southern intrusion of the Kuroshio Branch Current into the eastern part of

the Taiwan Strait (Fig. 4A) and mixing with the China coastal current. This is supported by the presence of the warm-water species *P. aculeatus* and the temperate-water species *C. sinicus* in the cluster of March 2000. Similar patterns concerning the enrichment of copepod communities due to Kuroshio Current were observed in the coastal area south of Japan (Noda *et al.*, 1998).

Nevertheless, it may be noticed that the indicator species for the transition phase between the two monsoon regimes should be carefully defined when we consider the entire northern subtropical waters of Taiwan because the spring season exhibited interannual variations in the northern sampling zone. The cluster gathering from Pali and the year 2002 (A12_2) only showed *T. turbinata* as an indicator species, whereas the cluster A10_2 was characterized by species including *Labidocera acuta*, *L. minuta*, *E. rimana* and *S. crassus*, as observed in the northern South China Sea (Hwang *et al.*, 2000a).

Calanoid copepods as indicators of the water masses

Many studies carried out all around the world reveal the influence of different hydrodynamic regimes on copepod communities. Along the northern coast of Argentina, copepod distribution patterns and their assemblages as part of the plankton community are greatly influenced by frontal hydrography (Berasategui *et al.*, 2006). The Californian copepod community of Baja changed substantially following trends in oceanographic conditions (Jimenez-Perez and Lavaniegos, 2004). The effect of the Kuroshio Current on the succession of the calanoid population has also been observed at smaller scale such as in Sagami Bay in Japan (Shimode *et al.*, 2006). In the aforementioned studies, the indirect impact of hydrographic events on biota (via variation in local climates, nutrient fluxes and primary production) was investigated to explain the distribution patterns of copepod species.

The cause of particular species' dominance is difficult to identify, because several interacting factors are usually involved and can greatly differ from one environment to the other. For quoting some external factors as examples, we have temperature, salinity, dissolved oxygen, food and predation. Moreover, life cycle duration, grazing, adaptation to cold or warm temperatures, or vertical migration, are distinct attributes for copepod species. They may differentially contribute to the selection of particular species that are adapted to a particular environment of an area at a particular time. It follows from this that species likely to co-occur should share advantageous life history traits that make them more successful. The community is simultaneously structured by a tension among abiotic and biotic

external forces (e.g. local conditions, temperature, turbulence and food concentration) and biotic internal forces (e.g. competition).

The present study does not provide information about the relative strengths of external and internal forcing. However, it does provide some clues about external forcing, here hydrodynamics, that induces the calanoid copepod assemblages to change, showing how the distribution patterns of indicator species may match hydrological conditions. Therefore, the present study has not only expanded our understanding of the dynamics of local Taiwan calanoid communities, but also provided further evidence of the influence of the physical environment on the species composition of copepod assemblages. Haury and Pieper (Haury and Pieper, 1988) affirmed that copepods can and do provide useful information about the dynamics of ecosystems. Within the same conceptual framework, previous studies have used variations in zooplankton composition and abundance as proxies to observe long-term changes in marine ecosystems (Rebstock, 2001, 2002; Beaugrand *et al.*, 2002; Lindley and Reid, 2002).

As part of the concept of species composition as an indicator of water masses, the present study has revealed parameters that should be considered. Previous local, descriptive studies carried out around Taiwan were assumed to confirm Boucher's proposition (Boucher, 1984; Boucher *et al.*, 1987) that such biological indicators can label water masses just as effectively as physical data (Lan *et al.*, 2004; Hsieh *et al.*, 2005). However, for the application of entire calanoid communities, the spatial and temporal scales over which the assemblages appear should be examined.

The difference in the assemblages between the two northern areas when separated or united exemplifies the caution that should be taken when generalizations are made across spatial scales. Areas presenting a strong coastal oceanic gradient in copepod diversity (Shih and Chiu, 1998) are exemplified not only around Taiwan, but also by the waters off Rio de Janeiro, southeast Brazil (Lopez *et al.*, 1999). Considerable differences between the clusters obtained from areas affected by the southwesterly monsoon (cluster 7 and cluster 11) also indicated that generalizations and extrapolations should be made with caution when characterizing indicator species common to both clusters. Both the period and the spatial origin were different for each of these clusters. Rezai *et al.* (Rezai *et al.*, 2005) suggested, moreover, that the calanoid copepod populations of the Strait of Malacca can be driven by interannual differences in the monsoons.

Furthermore, it is important to define the scales of the investigations properly, and additional studies are

needed on how to do this correctly. In the case of Taiwan waters, more thorough investigations around the southern and eastern parts of Taiwan are needed, that would include the effect of anthropogenic impacts in the highly urbanized northern part of Taiwan, but also studies of the biology of the enumerated indicator species. Validation *a posteriori*, combining the results of long-term monitoring programs and information from previously mentioned studies, could enhance the comparability of results and the modelling of events at global scale and across ecosystems.

ACKNOWLEDGEMENTS

This research was supported by Grants NSC 94-2621-B-019-001 and NSC 95-2621-B-019-002 from the National Science Council, ROC, and from the Center for Marine Bioscience and Biotechnology, National Taiwan Ocean University to J.S.H. The authors are indebted to Kao Tzu for providing some useful references and to Chih-Ming Lin for his priceless help in physical data acquisition. Thanks are extended to the captain, crew and technicians of the Ocean Researcher I, II, III and Fishery Researcher I for assistance on the different sampling cruises and to Marie Paul Gil, Hans-Uwe Dahms and Ian Jenkinson for their kind help in improvement of the language of this article. We finally thank the NCOR, Taiwan, for providing the satellite images to enhance the understanding of Taiwan coastal water hydrodynamics. The present work is part of the bilateral cooperation project selected in 2005 and 2006 from Taiwanese and French sides according to the bilateral agreements between the National Science Council, Taiwan (NSC 95-2621-B-019-002), and the Centre National de la Recherche Scientifique (CNRS, France). This work is a contribution to the co-tutorial PhD project of G.D. between the National Taiwan Ocean University, Taiwan, and the University of Sciences and Technologies of Lille, France.

REFERENCES

- Anneville, O., Souissi, S., Ibanez, F. *et al.* (2002) Temporal mapping of phytoplankton assemblage in Lake Geneva: annual and interannual changes in their patterns of succession. *Limnol. Ocean.*, **47**, 1355–1366.
- Anneville, O., Souissi, S., Gameter, S. *et al.* (2004) Seasonal and inter-annual scales of variability in phytoplankton assemblages: comparison of phytoplankton dynamics in three perialpine lakes over a period of 28 years. *Freshwater Biol.*, **49**, 98–115.
- Beaugrand, G., Reid, P. C., Ibanez, F. *et al.* (2002) Reorganization of North Atlantic marine copepod biodiversity and climate. *Science*, **296**, 1692–1694.
- Berasategui, A. D., Menu Marque, S., Gomez-Erach, M., Ramirez, F. C., Mianzan, H. W. and Acha, E. M. (2006) Copepod assemblages in a complex hydrographic region. *Estuar. Coast. Mar. Sci.*, **66**, 443–492.
- Boucher, M. (1984) Localization of zooplankton populations in the Ligurian marine front: role of ontogenic migration. *Deep-Sea. Res.*, **29**, 953–965.
- Boucher, M., Ibanez, F. and Prieur, L. (1987) Daily and seasonal variations in the spatial distribution of zooplankton populations in relation to the physical structure of the Ligurian Sea front. *J. Mar. Res.*, **45**, 133–173.
- Bradford, J. M. (1997) Distribution of the pelagic copepod *Temora turbinata* in New Zealand coastal waters, and possible trans-tasman population continuity. *NZ J. Mar. Freshwater Res.*, **11**, 131–144.
- Chang, W. B. and Fang, L. S. (2004) Temporal and spatial variations in the species composition, distribution, and abundance of copepods in Kaohsiung Harbor, Taiwan. *Zool. Stud.*, **43**(2), 454–463.
- Chen, Q. C. and Hwang, J. S. (1999) A new species of *Tortanus* (Copepoda calanoida) from Taiwan. *Crustaceana*, **72**, 265–271.
- Chen, Q. C. and Zhang, S. Z. (1965) The planktonic copepods of the Yellow Sea and the East China Sea I. Calanoida. *Stud. Mar. Sinica*, **7**, 265–271.
- Chen, Q. C., Hwang, J. S. and Yin, J. J. (2004) A new species of *Tortanus* (Copepoda, Calanoida) from the Nansha Archipelago of the South China Sea. *Crustaceana*, **77**, 129–135.
- Duffrene, M. and Legendre, P. (1997) Species assemblage and indicator species: the need for a flexible asymmetrical approach. *Ecol. Monogr.*, **67**, 345–366.
- Fang, K. L. and Yu, C. Y. (1981) A study of water masses in the seas of southernmost Taiwan. *Acta Oceanogr. Taiwanica*, **12**, 94–111.
- Frontier, S. and Pichod Viale, D. (eds) (1991) *Ecosystemes: Structure, Fonctionnement, Évolution*. Vol. 392
- Gomez, E., Echevarria, F., Garcia, C. M. *et al.* (2000) Microplankton distribution in the Strait of Gibraltar: coupling between organisms and hydrodynamics structures. *J. Plankton Res.*, **22**, 603–617.
- Gowen, R. J., Raine, R., Dickey-Colas, M. *et al.* (1998) Plankton distributions in relation to physical oceanographic features on the southern Malin Shelf, August 1996. *ICES J. Mar. Sci.*, **55**, 1095–1111.
- Hauray, L. R. and Pieper, R. E. (1988) Zooplankton: scales of biological and physical events. Soule, D. F. and Kleppel, G. S. (eds), In *Marine Organism as Indicators*. Springer-Verlag Press, New York.
- Hsiao, S. H., Lee, C. Y., Shih, C. T. *et al.* (2004) Calanoid copepods of the Kuroshio Current East of Taiwan, with Notes of the presence of *Calanus jashnovi* Hulsemann. *Zool. Stud.*, **43**, 323–331.
- Hsieh, C. H. and Chiu, T. S. (1998) Copepod abundance and species composition of the Tanshui river estuary and adjacent waters. *Acta Zool. Taiwanica*, **9**, 1–9.
- Hsieh, C. H., Chiu, T. S. and Shih, C. T. (2004) Copepod diversity and composition as indicators of intrusion of the Kuroshio Branch Current into the northern Taiwan Strait in Spring 2000. *Zool. Stud.*, **43**, 393–403.
- Hsieh, C. H., Chen, C. S. and Chiu, T. S. (2005) Composition and abundance of copepods and ichthyoplankton in Taiwan Strait (western North Pacific) are influenced by seasonal monsoons. *Mar. Fres. Res.*, **56**, 153–161.
- Hwang, J. S. and Turner, J. (1995) Behavior of cyclopoid, harpacticoid and calanoid copepods from coastal waters of Taiwan. *Mar. Ecol.*, **16**, 207–216.

- Hwang, J. S. and Wong, C. K. (2005) The China Coastal Current as a driving force for transporting *Calanus sinicus* (Copepoda Calanoida) from its population centers to waters of Taiwan and Hong Kong during the N.E monsoon period in winter. *J. Plankton Res.*, **27**, 205–210.
- Hwang, J. S., Chen, Q. C. and Wong, C. K. (1998) Taxonomic composition and grazing rate of calanoid copepods in coastal waters north of Taiwan. *Crustaceana*, **71**, 378–389.
- Hwang, J. S., Chen, Q. C., Lo, W. T. et al. (2000a) Taxonomic composition and abundance of the copepods in the north eastern South China Sea. *Natn. Taiwan Mus. Spec. Publ.*, **10**, 101–108.
- Hwang, J.-S., Wang, C.-H. and Chan, T.-Y. (eds) (2000b) Proceedings of the international symposium on marine biology in Taiwan-Crustacean and zooplankton taxonomy, ecology and living resources, 26–27 May, 1998, Taipei, Taiwan. *Nat. Taiwan Mus. Spec. Publ.*, **10**, 199.
- Hwang, J. S., Chen, Q. C. and Wong, C. K. (2003) Taxonomic composition, density and biomass of calanoid copepods in coastal waters of south-western Taiwan. *Crustaceana*, **76**, 196–206.
- Hwang, J. S., Ho, J. S. and Shih, C. T. (eds) (2004a) Proceeding of the 8th International Conference on Copepoda. *Zool. Stud.*, **43**, 1–510.
- Hwang, J.-S., Tu, Y.-Y., Tseng, L.-C. et al. (2004b) Taxonomic composition and seasonal distribution of copepod assemblages from waters adjacent to nuclear power plant I and II in Northern Taiwan. *J. Mar. Sci. Tech.*, **12**, 380–391.
- Hwang, J. S., Souissi, S., Tseng, L. C. et al. (2006) A 5-year study of the influence of the northeast and southwest monsoons on copepod assemblages in the boundary coastal waters between the East China Sea and the Taiwan Strait. *J. Plankton Res.*, **28**, 943–958.
- Jan, S. and Chao, S. Y. (2002) Seasonal variation of volume transport in the major inflow region of the Taiwan Strait: the Penghu channel. *Deep-Sea Res. II*, **50**, 1117–1122.
- Jan, S., Chern, C. S. and Wang, J. (1995) A numerical study on currents in Taiwan Strait during summertime. *La Mer*, **33**, 23–40.
- Jan, S., Wang, J., Chern, C. S. et al. (2002) Seasonal variation of the circulation in the Taiwan Strait. *J. Mar. Syst.*, **35**, 249–268.
- Jiménez-Pérez, L. C. and Lavaniegos, B. E. (2004) Changes in dominance of copepod off Baja California during the 1997–1999 El Niño and la Niña. *Mar. Ecol. Prog. Ser.*, **277**, 147–165.
- Kouwenberg, J. H. M. (1994) Copepod distribution in relation to seasonal hydrodynamic and spatial structure in the northwestern Mediterranean (Golfe du Lion). *Estuarine Coastal Shelf. Sci.*, **38**, 69–90.
- Lan, Y. C., Shih, C. T., Lee, M. A. and Shieh, H. Z. (2004) Spring distribution of copepods in relation to water masses in the northern Taiwan Strait. *Zool. Stud.*, **43**, 332–343.
- Lee, H. J. and Chao, S. Y. (2003) A climatological description of circulation in and around the East China Sea. *Deep-Sea Res. II*, **35**, 249–268.
- Lee, M. A., Chang, Y. I., Sakaida, F. et al. (2005) Validation of satellite-derived sea surface temperatures for waters around Taiwan. *TAO*, **16**(5), 1189–1204.
- Liang, W. D., Tang, T. Y., Yang, Y. J. et al. (2003) Upper-ocean currents around Taiwan. *Deep-Sea Res. II*, **50**, 1085–1106.
- Lin, S. and Li, S. (1991) Reproductive rates of a marine planktonic copepod *Labidocera euchaeta* Giesbrecht in Xiamen Harbor. *Chin. J. Ocean. Limn.*, **9**, 319–328.
- Lin, C. L. and Ho, J. S. (1998) Two new species of ergasilid copepods parasitic on fishes cultured in brackish water in Taiwan. *Proc. Biol. Soc. Wash.*, **111**, 15–27.
- Lindley, J. A. and Reid, P. C. (2002) Variations in the abundance of *Centropages typicus* and *Calanus helgolandicus* in the North Sea: deviations from close relationships with temperature. *Mar. Biol.*, **141**, 153–165.
- Liu, K. K., Gong, G. C., Pai, C. Z. et al. (1992) Response to the Kuroshio upwelling to the onset of the northeast monsoon in the sea north of Taiwan, observation and a numerical simulation. *J. Geo. Res.*, **97**, 12511–12526.
- Liu, K. K., Peng, T. H., Shaw, P. T. et al. (2003) Circulation and biogeochemical processes in the East China Sea and the vicinity of Taiwan: an overview and a brief synthesis. *Deep-Sea Res. II*, **50**, 1055–1064.
- Lo, W. T., Shih, C. T. and Hwang, J. S. (2001) Identity and abundance of surface dwelling, coastal copepods of south-western Taiwan. *Crustaceana*, **74**, 1139–1157.
- Lo, W. T., Chung, C. L. and Shih, C. T. (2004a) Seasonal distribution of copepods in Tapong bay, Southwestern Taiwan. *Zool. Stud.*, **43**, 464–474.
- Lo, W. T., Hwang, J. S. and Chen, Q. C. (2004b) Spatial distribution of copepods in surface waters of the southeastern Taiwan Strait. *Zool. Stud.*, **43**, 218–228.
- Lo, W. T., Shih, C. T. and Hwang, J. S. (2004c) Diel vertical migration of the planktonic copepods at an upwelling station North of Taiwan. Western north pacific. *J. Plankton Res.*, **26**, 89–97.
- Lopez, R. M., Brandini, F. P. and Gaeta, S. A. (1999) Distribution pattern of epipelagic copepods off Rio de Janeiro (SE Brasil) in summer 1991/1992 and winter 1992. *Hydrobiologia*, **411**, 161–174.
- Mauchline, J. (1998) The biology of calanoid copepod. In Blaxter, J. F. S., Southward, A. J. and Tyler, T. A. (eds.), *Advance in Marine Biology*. Vol. **33**. Elsevier Academic Ltd. Press, London.
- Noda, M., Ikeda, I., Ueno, S., Hashimoto, H. and Gushima, K. (1998) Enrichment of coastal zooplankton communities by drifting zooplankton patches from the Kuroshio front. *Mar. Ecol. Prog. Ser.*, **176**, 55–65.
- Petraitis, P. S. and Latham, R. E. (1999) The importance of scale in testing the origins of alternative community states in ecosystems. *Ecology*, **80**, 429–442.
- Rebstock, G. A. (2001) Long term stability of species composition in calanoid copepod populations off southern California. *Mar. Ecol. Prog. Ser.*, **215**, 213–224.
- Rebstock, G. A. (2002) Climatic regimeshifts and decadal-scale variability in calanoid copepod populations off southern California. *Glob. Change Biol.*, **8**, 71–89.
- Rezai, H., Yusoff, F. M., Arshad, A. and Ross, O. (2005) Spatial and temporal variations in calanoid copepod distribution in the Straits of Malacca. *Hydrobiologia*, **537**, 157–167.
- Sanders, R. W. (1987) Tintinnids and other microzooplankton—seasonal distributions and relationships to resources and hydrography in a Maine estuary. *J. Plankton Res.*, **9**, 65–77.
- Shih, C. T. and Young, S. S. (1995) A checklist of free-living copepods, including those associated with invertebrates, reported from the adjacent seas of Taiwan. *Acta Zool. Taiwanica*, **6**, 64–81.
- Shih, C. T. and Chiu, T. S. (1998) Copepod diversity in the water masses of southern East China Sea north of Taiwan. *J. Mar. Syst.*, **15**, 533–542.

- Shih, C. T., Hwang, J. S. and Huang, W. B. (2000) Planktonic copepods from an upwelling station north of Taiwan, western North Pacific. *Nat. Mus. Taiwan Spec. Publ.*, **10**, 19–35.
- Shimode, S., Toda, T. and Kikuchi, T. (2006) Spatio-temporal changes in diversity and community structure of planktonic copepods in Sagami Bay, Japan. *Mar. Biol.*, **148** (3), 581–597.
- Souissi, S., Ibanez, F., Ben Hamadou, R. *et al.* (2001) A new multivariate mapping method for studying species assemblages and their habitats: examples using bottom trawl surveys in the Bay of Biscay (France). *Sarsia*, **86**, 527–542.
- Strickler, J. R. and Hwang, J. S. (1999) Matched spatial filters in long working distance microscopy of phase objects. In Wu, J. L., Hwang, P. P., Wong, G., Kim, H. and Cheng, P. C. (eds), *Focus on Multidimensional Microscopy*, Vol. **2**, World Scientific Publishing Co., Singapore, pp. 217–239.
- Takahashi, T. and Hirakawa, K. (2001) Day–night vertical distribution of the winter and spring copepod assemblages in Toyama Bay, Southern Japan Seas, with special reference to *Metridia pacifica* and *Oithona atlantica*. *Bull. Plankton Soc. Jap.*, **48**, 1–13.
- Tseng, R. S. and Shen, Y. T. (2003) Lagrangian observations of surface flow patterns in the vicinity of Taiwan. *Deep-Sea Res. II*, **50**, 1107–1116.
- Turner, J. T. (2004) The importance of small planktonic copepods and their roles in pelagic marine food webs. *Zool. Stud.*, **43**, 255–266.
- Wong, C. K., Hwang, J. S. and Chen, Q. C. (1998) Taxonomic composition and grazing impact of calanoid copepods in coastal waters near nuclear power plants in northern Taiwan. *Zool. Stud.*, **37**(4), 330–339.
- Wong, G. T. F., Chao, S. Y., Li, Y. H. *et al.* (2000) The Kuroshio Edge Exchange Processes (KEEP) Study—an introduction to hypotheses and highlights. *Cont. Shelf Res.*, **20**, 335–347.
- Wu, C. H., Hwang, J. S. and Yang, J. S. (2004) Diet of three copepods (Poecilostomatoida) in the southern Taiwan Strait. *Zool. Stud.*, **43**, 388–392.
- Wyrki, K. (1961) Physical oceanography of the southeast Asia waters. Scripps Institute of Oceanography NAGA 195.
- Zheng, Z., Li, S. J. and Chen, B. Y. (1992) On the distribution of planktonic copepods in Taiwan strait. *Taiwan Strait*, **1**, 69–79.